Department of Hydraulic and Environmental Engineering
The Norwegian University of Science and Technology

Class notes:

Computational Fluid Dynamics in Hydraulic and Sedimentation Engineering

by Nils Reidar B. Olsen

Foreword

From 1991 to 1998 I was teaching CFD as a part of post-graduate classes in hydro-power engineering at Department of Hydraulic and Environmental Engineering at the Norwegian University of Science and Technology. The content of CFD in the classes had been increasing over the years, reflecting the new possibilities for solving practical problems with computers. The main application has been to calculate the trap efficiency of sand traps and reservoirs, and to investigate flow pattern with regards to hydropower intakes. This has reflected both the focus of the teaching and also the tutoring of Ph.D. and MS students using CFD in their projects.

When teaching CFD, I initially relied largely on papers and selected notes from relevant books. There was not any textbook to follow, and this was problem for the students. In the spring of 1997 Prof. D. K. Lysne asked be to write these class notes. Hopefully, the notes will be improved over the years, and be of help to students trying to learn CFD.

The target group for this document is students in hydraulic and sedimentation engineering. The prerequisite is some knowledge of processes in fluid flow and differential equations, for example basic classes in hydraulics/fluid mechanics and mathematics, at an undergraduate university level.

I want to thank Dagfinn K. Lysne, Catherine A. M. E. Wilson, Tor Håkon Bakken and Hilde Marie Kjellesvig for valuable comments to the text.

Provided the document is not changed, it may freely be copied and distributed.

Nils Reidar Olsen

Table of content

1. Background for CFD in hydraulic and sedimentation engineering

Computational Fluid Dynamics (CFD) is the science about calculation of fluid flow and related variables using a computer. Usually the fluid body is divided into cells or elements forming a grid. Then equations for unknown variables are solved for each cell. This requires a substantial amount of computing resources. Therefore, this science has not progressed to a practically applicable stage until recently. In coming years, CFD will increasingly be used in hydraulic and sedimentation engineering. It is therefore important that engineering students are given insight into this topic.

This document describes the solution techniques based on the control volume method. Particular emphasis is put on calculation of sediment transport, and also on water flow with free surface. This is in accordance with the class in Sedimentation Engineering taught at the Institute of Hydraulic and Environmental Engineering of the Norwegian University of Science and Technology.

Problems related to hydraulics and sedimentation engineering have previously often been solved by the use of physical models. Physical models are costly and time-consuming, compared with CFD models. A particular problems with physical model studies has been the simulation of suspended sediments. Cohesive forces are present for fine particles necessary when scaling down sediment sizes for simulation of sand traps. Calculation of trap efficiency of sand traps is one of the first areas where numerical models were used instead of physical models. Since then the CFD models have expanded to include sediment transport with time-dependent moveable bed, trap efficiency, deposition, erosion, local scour, turbidity currents, flood waves, spillways and head loss in channels and tunnels.

2. Grids

A basic concept of CFD is to divide the fluid geometry into elements or cells, and then solve an equation for each cell. In the following text, the word cell will be used instead of element, to avoid confusion with the finite element method. The algorithms described in the following chapters are based on the finite volume method, except Chapter 5, giving a short introduction to the finite element method.

2.1 Classifications

Grids can be classified according to several characteristics:

- shape
- orthogonality
- structure
- blocks
- position of variable
- grid movements

The **shape** of the cells is usually triangular or quadrilateral:
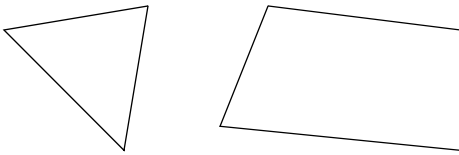
Triangular and quadrilateral shapes

The **orthogonality** of the grid is determined by the angle between crossing grid lines. If the angle is 90 degrees, the grid is orthogonal. If it is different from 90 degrees, the grid is non-orthogonal.
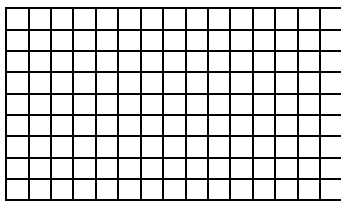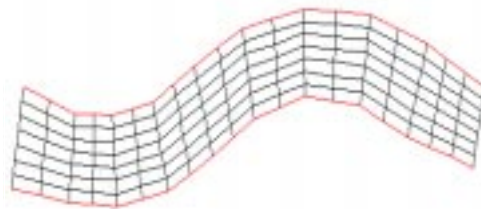
Orthogonal grid   *Non-orthogonal grid*

For non-orthogonal grids, a non-orthogonal coordinate system is often used to derive terms in the equations. The coordinates then follow the grid lines of a structured grid. The three non-orthogonal coordinate lines are often called ξ,ψ,ζ, corresponding to x,y

and z in the orthogonal coordinate system. This is also shown on the figure below:

ζ

z

ψ

y

Non-orthogonal coordi-nate system following the grid lines.

ξ

x
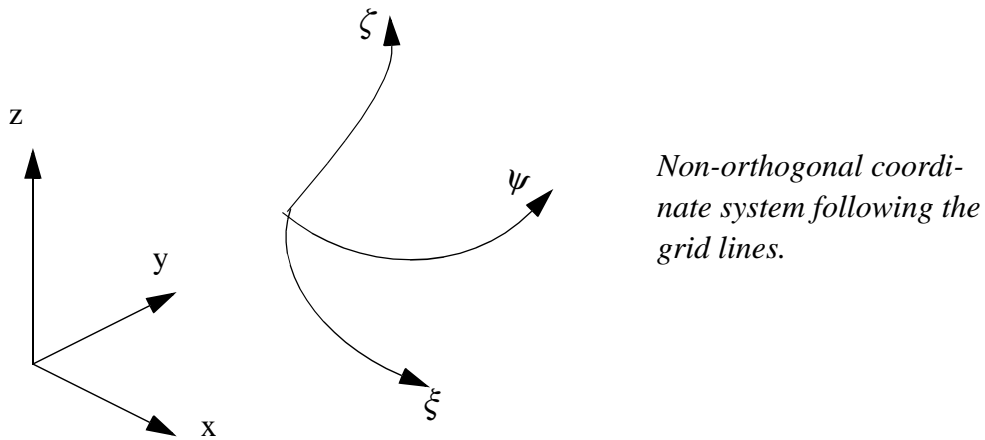
Grids can be **structured** or non-structured. Often a structured grid is used in finite volume methods and an unstructured grid is used in finite element methods. However, this is not always the case. The figure below shows a structured and an unstructured grid. In a structured grid it is possible to make a two-dimensional array indexing the grid cells. If this is not possible, the grid is unstructured.

Unstructured grid
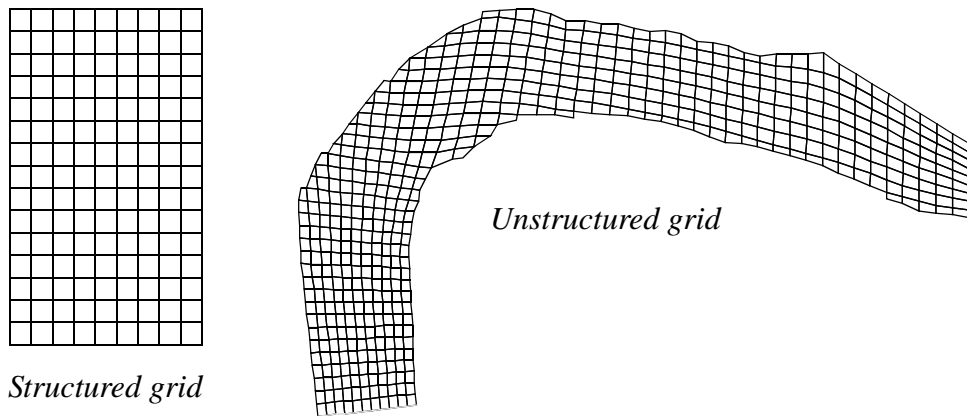
Structured grid

Almost all grids using triangular cells are unstructured.

A **multi-block** grid is a made from several structured grids as shown on the figure to the right:
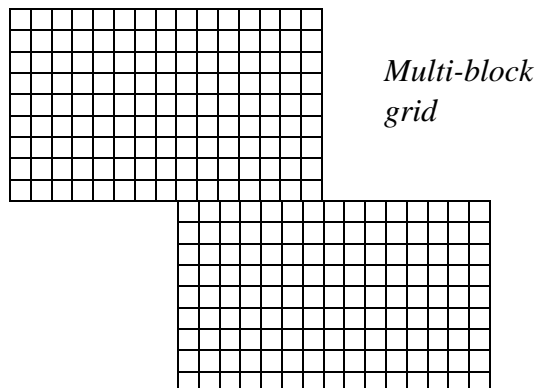
There are also classifications according to where in the grid the variable is calculated. To improve stability, some models calculate pressure and velocity in different positions. This is called a **staggered**

Multi-block grid

grid. A **non-staggered** grid is used when all variables are calculated in the same location, most often the centre of each cell. These terms are most often used in the control volume terminology. In finite element methods, the variables are most often calculated at grid intersections, and sometimes also in the centre of a cell. The following figure shows this with circles indicating the locations of the calculation points. P denotes a point where pressure is calculated, and U denotes a point where velocity is calculated.

P U→ P U→ P	*Staggered grid*
U,P→ U,P→ U,P→	*Non-staggered grid*
U,P U,P U,P U,P U,P U,P U,P U,P U,P U,P U,P	*Finite element variable layout*

An **adaptive** grid moves according to the calculated flow field or the physics of the problem. When the water surface or the bed moves during a time step, it is possible to make the grid move accordingly, to calculate the situation for the new geometry. Thereby time-dependent calculations of bed changes and water levels can be done.

An adaptive grid is used to model bed changes in for example sediment deposition, reservoir flushing or local scour. It is also used to model changes in the water surface when for example calculating a flood wave.
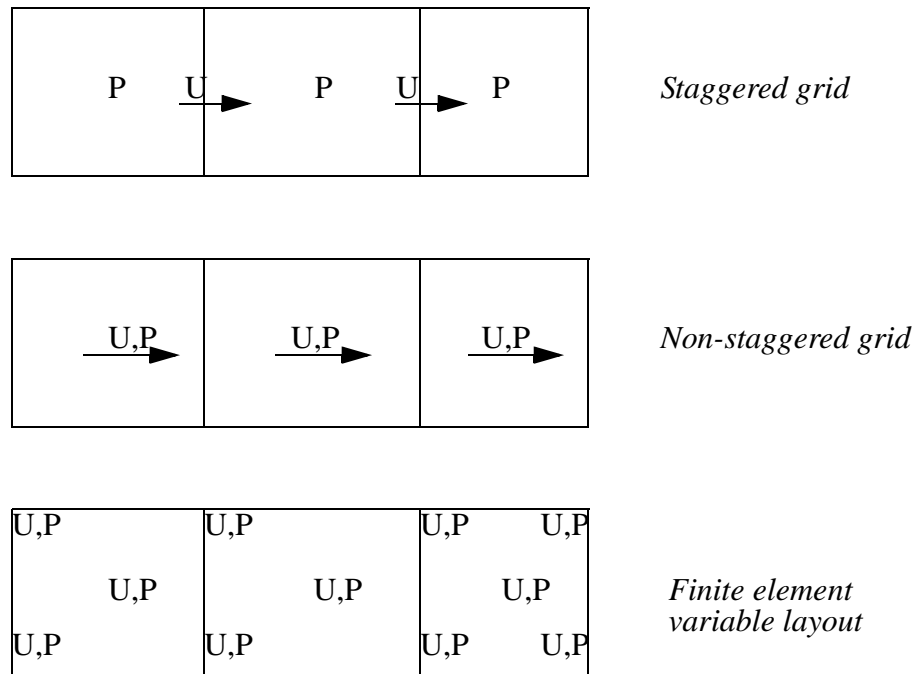
2.2 Structured grid numbering

There are several ways to identify cell and grid lines in a structured grid. When using some CFD programs, it is important to know the numbering system for each particular program in order to identify the regions of inflow/outflow and outblocking procedures. The numbering system described in the following is used by the SSIIM program.

In a structured grid, there will always be one more grid line than grid cells in any given direction. Because boundary conditions are also needed, there will be a grid cell with zero thickness at the walls. The number of this cell is 1. The number of the first cell

inside the grid is therefore 2. The figure below shows a two-dimensional view of the grid, with numbers.

(1,3)	(2,3)	(3,3)	(4,3)
(1,2)	(2,2)	(3,2)	(4,2)
(1,1)	(2,1)	(3,1)	(4,1)

Grid line numbering

(2,3)	(3,3)	(4,3)
(2,2)	(3,2)	(4,2)

Grid cell numbering
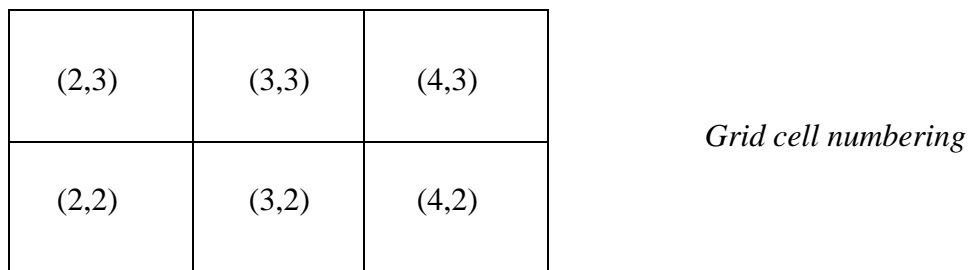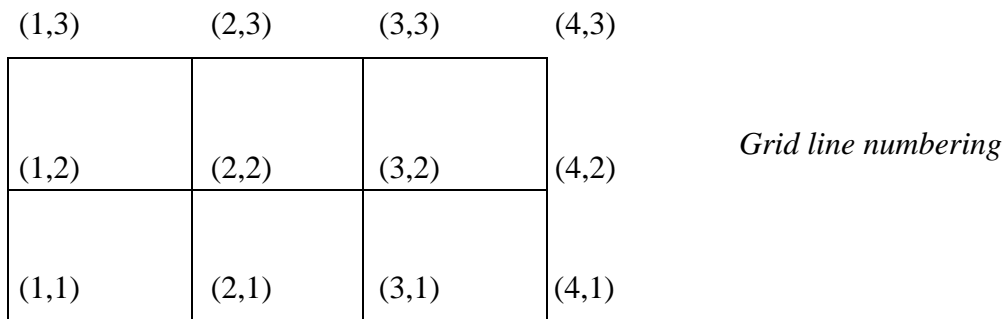
The variable in centre of the "first" grid cell has number (2,2). The variables on the boundary are only used as boundary conditions. The variables in the corners: (1,1), (1,5), (5,1) and (5,5) are not used for anything.

Note that different computer programs may have different grid numbering systems.

2.3 Grid qualities

The accuracy and convergence of a finite volume calculation depends on the quality of the grid. Three grid characteristics are important:

- non-orthogonality
- aspect ratio
- expansion ratio

The non-orthogonality of the grid line intersections is the deviation from 90 degrees. If the grid line intersection is below 45 degrees or over 135 degrees, the grid is said to be very non-orthogonal. This is a situation one should avoid. Low non-orthogonality of the grid leads to more rapid convergence, and in some cases better accuracy.

The aspect ratio and expansion ratio is described in the figure below:

The figure shows two grid cells, *A* and *B*. The length of the cells are Δx_A and Δx_B.

Expansion/aspect ratio
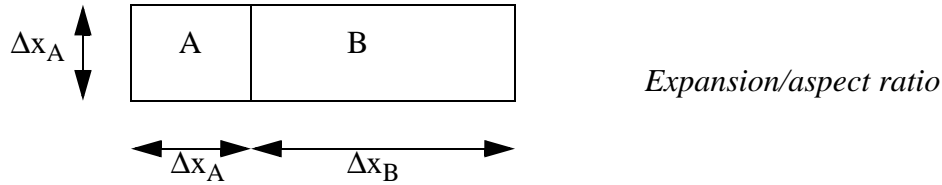
The **expansion ratio** of the grid at these cells is $\Delta x_A/\Delta x_B$.

The **aspect ratio** of the grid at cell A is $\Delta x_A/\Delta y_A$.

The expansion ratio and the aspect ratio of a grid should not be too great, in order to avoid convergence problems and inaccuracies. Aspect ratios of 2-3 should not be a problem if the flow direction is parallel to the longest side of the cell. Experience shows that aspect ratios of 10-50 will give extremely slow convergence for water flow calculations. Expansion ratios under 1.2 will not pose problems for the solution. Experience also shows that expansion ratios of around 10 can give very unphysical results for the water flow calculation.

2.4 Elliptic grid generation

Elliptic grid generation is a method to distribute internal points smoothly in a structured quadrilateral grid. This is done by solving a Laplace or Poisson equation for the location of the grid line intersections:

$$\nabla^2 \xi^i = P^i \qquad\qquad (2.4.1)$$

The location of the grid lines are denoted ξ. P is a source term used for attracting grid lines to a side or a point.

An example of using elliptic grid generation is given below:
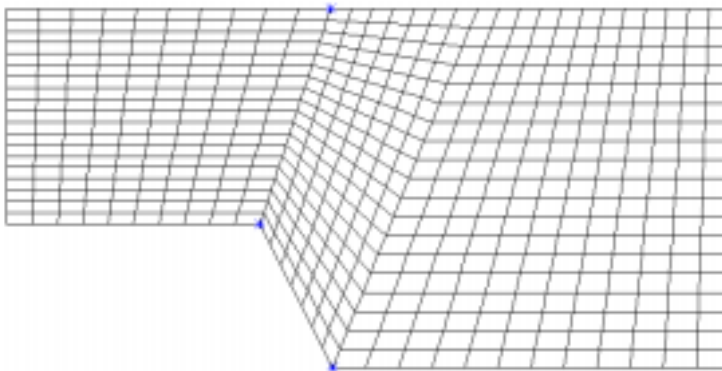
This grid is made by use of transfinite interpolation. This means that straight lines are made between the points on the wall.

10
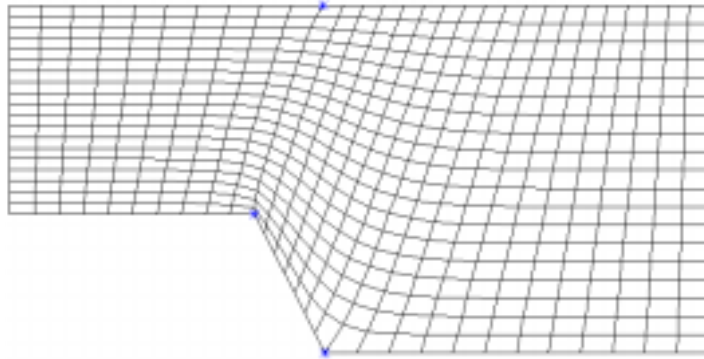
Elliptic procedures are used to obtain the grid shown above, with no attractions. This means P=0 for Equation 4.2.1.
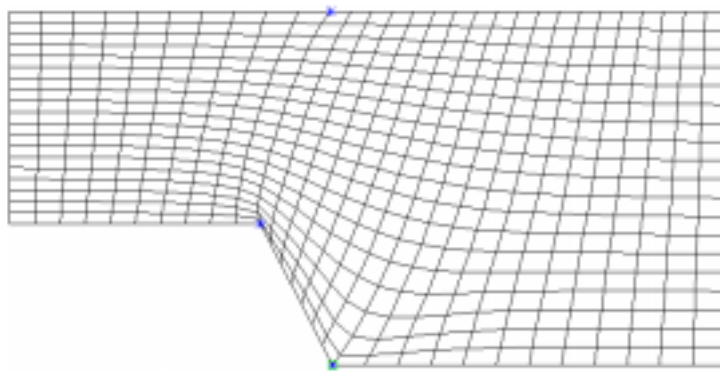
Looking at the lower point of the step, the cells are smaller closer to the wall. This is due to attraction functions. $P \neq 0$ for Equation 4.2.1.

2.5 Practical advice for generating structured non-orthogonal grids

Making a good grid is a considerable part of the work for CFD calculations for complex geometries. Experience seems to be very important for this task, so the first advice is to practice making grids.

Before starting to make the grid, some information is necessary:

1. How many grid cells are available for the grid? This can be calculated from the capacity of the computer and the expected computational time.
2. Drawings of the geometry are important, where boundaries and the inflow/outflow regions are shown together with possible islands or other **outblocked** regions.

An **outblocked** region is a part of the grid where water is not allowed to flow. It can be used for making islands or obstacles in the flow. An example is given below with flow around a square obstacle:
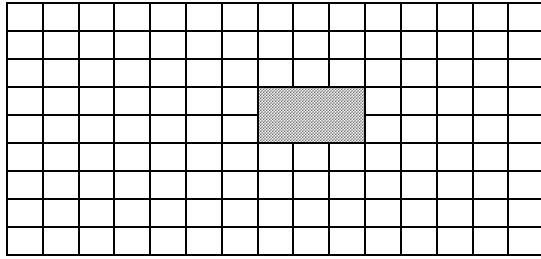
Grid with an outblocked region of 3x2 cells

Note that not all computer programs have the option of blocking out parts of the grid.

If the geometry is complex, one should make a paper sketch of the grid before starting to use the computer. The paper sketch should be reasonably large in order for the details to be visible. The boundary of the grid should be marked with one colour, and inflow/outflow regions with another colour.

One should start with deciding the general structure of the grid: where the four sides of the grid should be located. If outblocking is needed and possible, this should be decided together with the location of the outblocking in the grid. Then one should start drawing the grid, using a pencil and an eraser, as modifications are always needed.

One should preferably start making a very coarse grid, maybe with only 6-12 cells, and making the grid finer afterwards. When drawing the grid, the following points should be kept in mind:

1. The grid lines should follow the stream lines as much as possible
2. The grid line intersections should be as orthogonal as possible
3. The grid aspect ratio should not be too great
4. The grid expansion ratio should not be too great
5. There should be higher grid densities in areas with high velocity/concentration gradients. In a not too complex part of a river, the gradients in cross-streamwise direction are larger than in the streamwise direction. The grid cells can then be longer in the streamwise direction than in the cross-streamwise direction. An example is given in the figure below, where the aspect ratio for the cells are above unity.
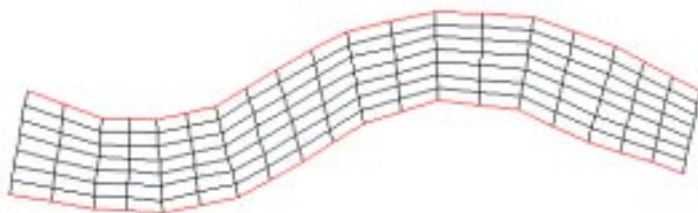
After having made the paper sketch of the grid, the tools of the CFD computer program can be used to make the final grid. Note that the same points as given above apply when using the grid tools of the CFD program.

2.6 Exercises

The following three line styles are used in the sketches in the problems:

Inflow   Outflow   Wall

Problem 2.1

Make a sketch of a 2D structured non-orthogonal grid with 300 cells for the geometry given below.
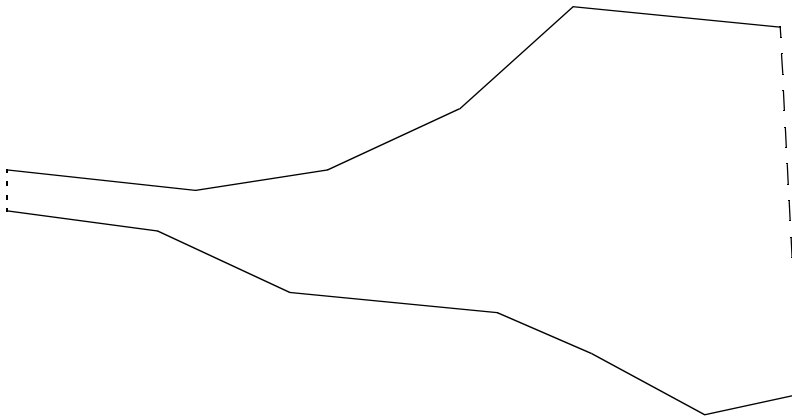
Problem 2.2

Make a sketch of a 2D structured non-orthogonal grid with 300 cells for the geometry given below, without using outblocking.
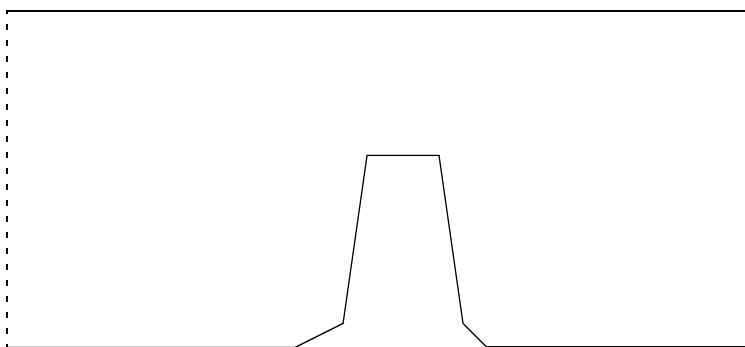
Problem 2.3

Make a sketch of a structured non-orthogonal grid with 300 cells for the geometry given below, but use outblocking for the groyne.
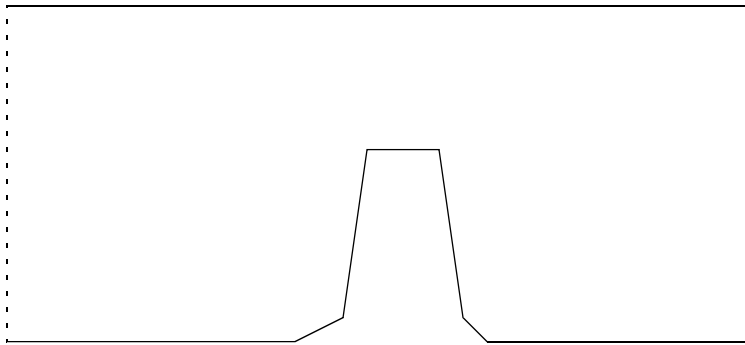
Problem 2.4

Make a sketch of a structured non-orthogonal grid with 500 cells for the geometry given below. You may use outblocking.
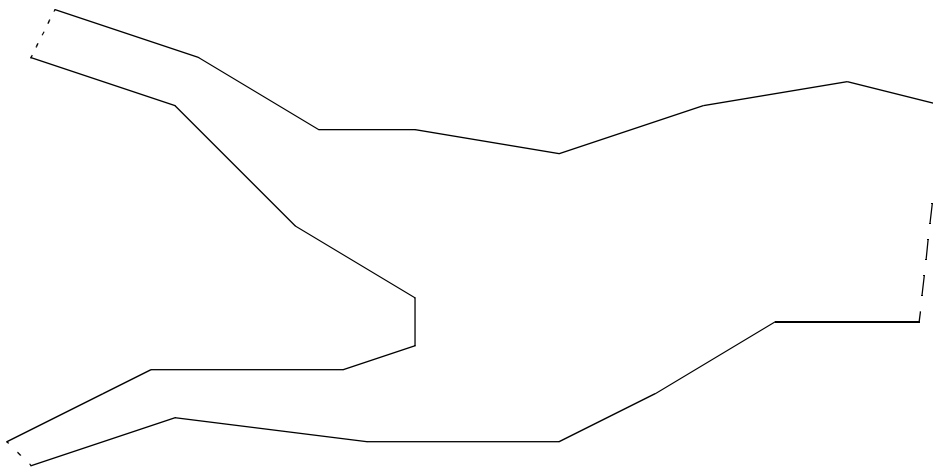
Problem 2.5

Make a sketch of a structured non-orthogonal grid with 600 cells for the geometry given below.
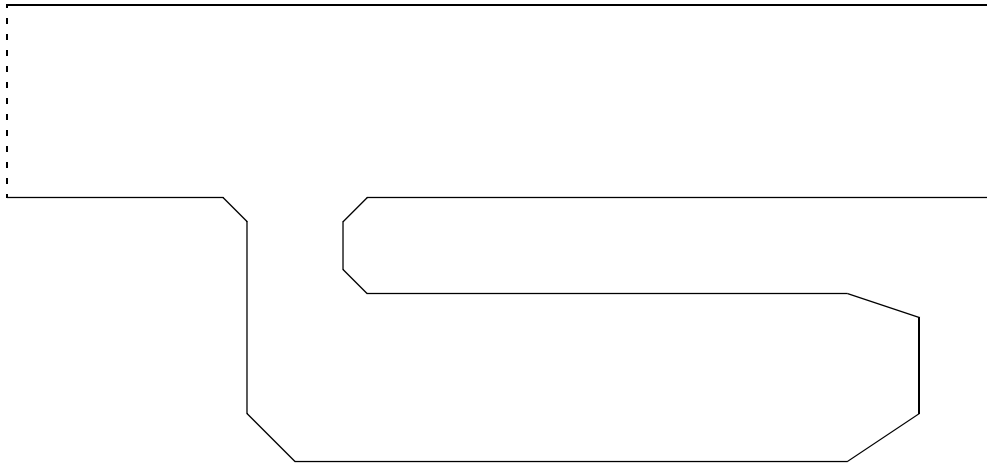
Problem 2.6

Make a paper sketch of a structured non-orthogonal grid with 2000 cells for a circular cylinder with diameter 1.0 meters placed vertically in the centre of a 4 meter wide and 10 meter long flume.

Problem 2.7

Use a CFD grid editing program and make the grid of Problem 2.6, with the aid of an elliptic grid generator. Do not use attraction functions.

Problem 2.8

Repeat the grid generation procedure of Problem 2.7, but use attraction functions to make the grid denser close to the anticipated gradients in flow.

3. Calculation of sediment transport

This chapter describes methods to calculate suspended sediment transport in a water flow. The same methods can be used to calculate other parameters, for example water quality constituents, temperature etc. It is often easier to understand the physics of the problem when the unknown variable is a concentration of particles. Fluxes through cell surfaces are easier to understand when one can imagine particles drifting with the water through the cell surfaces.

The transport processes are described first, and then the numerical algorithms are described. Note that the numerical methods described in this chapter are also used for calculation of the water velocity field. However, thinking about this makes it more difficult to understand the methods, so the student should study this chapter first, and then move to Chapter 4 afterwards, to learn more about the velocity field calculation.

3.1 Transport processes

There are two main transport processes for suspended sediment transport: convection and diffusion. The convection of sediments is the transport by the average water velocity. The transport because of the fall velocity of the sediments is also a type of convective transport. When calculating the flux, F, through a given surface with area A, the following formula is used:

$$F = c * U * A \qquad (3.1.1)$$

U is the average velocity of the sediments normal to the surface, and c is the average sediment concentration over the area. The sediment velocity will be the sum of the water velocity and the sediment fall velocity.

As an example, we can look at a uniform flow, with zero vertical water velocity. If the surface is vertical, the sediment fall velocity component is zero normal to the surface. Then the velocity U will be equal to the horizontal water velocity. If the surface is parallel to the bed/water surface, then the water velocity component normal to the surface will be zero. The velocity U in Formula 3.1.1 will then be equal to the fall velocity of the sediment particles.

The other process is the turbulent diffusion of sediments. This is due to turbulent mixing and concentration gradients. The turbulent mixing process is usually modelled with a turbulence mixing coefficient, Γ, defined as the sediment flux divided by the concentration gradient:

$$\Gamma = \frac{\left(\dfrac{F}{A}\right)}{\left(\dfrac{dc}{dx}\right)} \qquad (3.1.2)$$

Normally, the convective transport will be dominating. But in some cases, the diffusive transport is important. An example is the reduced settling in a sand trap because of turbulence.

The processes and Formulas 3.1.1 and 3.1.2 will be used extensively in the following description of the finite volume method.

3.2 The convection-diffusion equation

The convection-diffusion equation for steady sediment transport is:

$$U_j \frac{\partial c}{\partial x_j} + w \frac{\partial c}{\partial z} = \frac{\partial}{\partial x_j}\left(\Gamma_T \frac{\partial c}{\partial x_j}\right) \qquad (3.2.1)$$

The sediment concentration is denoted c, w is the fall velocity of the particles, U is the water velocity, x is a space dimension and Γ is the turbulent diffusivity. The three directions are x_1, x_2 and x_3, and the velocities in the three directions are U_1, U_2 and U_3.

The Einstein summation convention/tensor notation is used, meaning repeated indexes are summed over all directions. For three-dimensional flow this means that the equation can be written:

$$U \frac{\partial c}{\partial x} + V \frac{\partial c}{\partial y} + W \frac{\partial c}{\partial z} + w \frac{\partial c}{\partial z} = \frac{\partial}{\partial x}\left(\Gamma_T \frac{\partial c}{\partial x}\right) + \frac{\partial}{\partial y}\left(\Gamma_T \frac{\partial c}{\partial y}\right) + \frac{\partial}{\partial z}\left(\Gamma_T \frac{\partial c}{\partial z}\right) \quad (3.2.2)$$

Here, x, y and z are used in the tree directions instead of x_1, x_2 and x_3, and U, V and W are used instead of U_1, U_2 and U_3.

Equation 3.2.2 is used to describe the process of sediment transport. It is used in papers and documentation, but it is not manipulated mathematically or used in any practical way in the numerical modelling described here.

3.3 Discretization methods

The discretization described here is by the control volume method.

The main point of the discretization is:

To transform the partial differential equation into a new equation where the variable in one cell is a function of the variable in the neighbour cells

The new function can be thought of as a weighted average of the concentration in the

17

neighbouring cells. For a two-dimensional situation, the following notation is used, according to directions north, south, east and west:

:

    c_n concentration in cell n

    c_e concentration in cell e

    c_s concentration in cell s

    c_w concentration in cell w

    c_p concentration in cell p
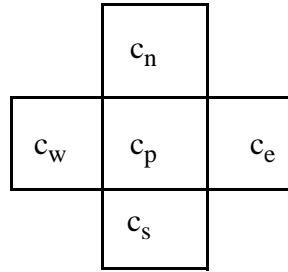
a_e : weighting factor for cell e

a_w : weighting factor for cell w

a_n : weighting factor for cell n

a_s : weighting factor for cell s

$a_p = a_e + a_w + a_n + a_s$

The formula becomes:

$$c_p = \frac{a_w c_w + a_e c_e + a_n c_n + a_s c_s}{a_p} \qquad (3.3.1)$$

The weighting factors for the neighbouring cells a_e, a_w, a_n and a_s are often denoted a_{nb}

What we want to obtain are formulas for a_{nb}.

There are a number of different discretization methods available for the control-volume approach. The difference is in *how the concentration on a cell surface is calculated*. Some methods are described in the following.

3.4 The First-Order Upstream Scheme

This method is also called the First-Order Upwind Scheme, as it was developed first for situations with air flow.

For a non-staggered grid, the values of the variables are given in the center of the cells. Using the finite volume method, it is necessary to estimate variable values on the cell surfaces. The main idea of the upstream methods is to estimate the surface value from the *upstream* cell. The first order method uses information in only one cell upstream of the cell surface. In other words: the concentration at a cell surface for the first-order upstream method is the same as the concentration in the cell on the upstream side of the cell side.

The control volume method is based on continuity of sediments. The basis of the calculation is the fluxes on a cell surface. The surface area is denoted A; the velocity at the surface, normal to it, is denoted U; c is the concentration at the surface, and Γ is the turbulent diffusion at the surface.

The convective flux is calculated as: $U * A * c$

The diffusive flux is calculated as: $\Gamma * A * dc / dx$

The term *dc/dx* is calculated as the concentration difference between the cells on each side of the surface, divided by the distance between the centres of the cells. Looking at the west side of cell *p*, the following figure explains the variables:
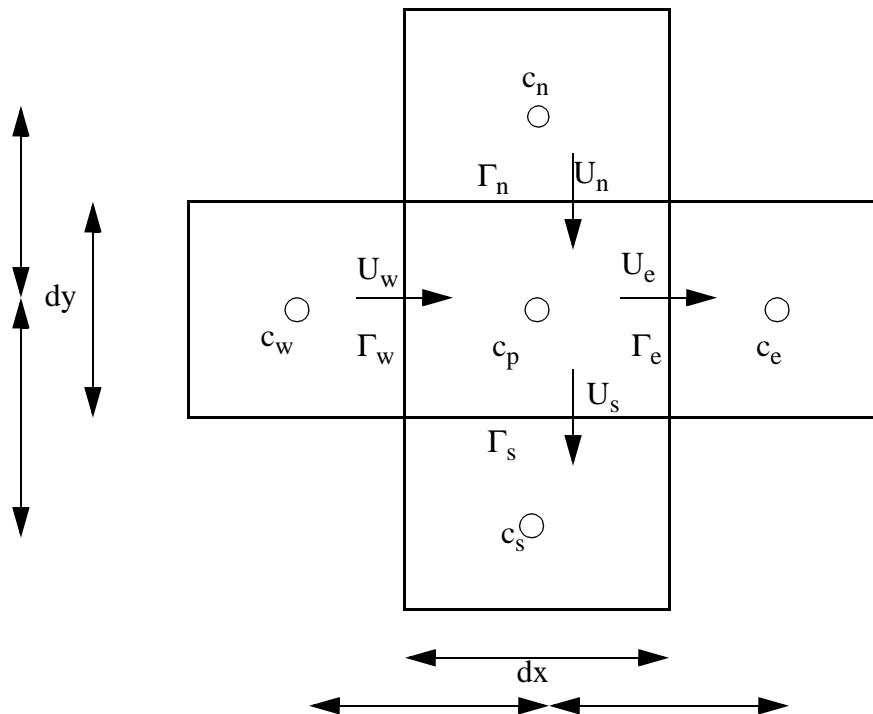
The flux, *F*, through the west side of cell *P* then becomes:

West side: $F_w = U_w A_w c_w + \Gamma_w A_w (c_w - c_p) / dx$

where A_w is the area of the cell wall on the west side, equal to Δy times the height of the wall. For the other sides, the following fluxes are obtained:

East side: $F_e = U_e A_e c_p + \Gamma_e A_e (c_p - c_e) / dx$
North side: $F_n = U_n A_n c_n + \Gamma_n A_n (c_n - c_p) / dy$
South side: $F_s = U_s A_s c_p + \Gamma_s A_s (c_p - c_s) / dy$

The sum of the fluxes is zero, in other words: Fw-Fe+Fn-Fs = 0. This gives the following equation:

$$(\Gamma_e A_e / dx + U_e A_e + \Gamma_w A_w / dx + \Gamma_n A_n / dy + U_s A_s + \Gamma_s A_s / dy) c_p =$$
$$\Gamma_e A_e / dx \, c_e + (U_w A_w + \Gamma_w A_w / dx) c_w +$$
$$\Gamma_s A_s / dy \, c_s + (U_n A_n + \Gamma_n A_n / dy) c_n \qquad\qquad (3.4.1)$$

When we compare Equation 3.3.1 with Equation 3.4.1, we see they are the same. The concentration in cell *P* is a function of the concentration in the neighbouring cells. The resulting weighting factors are:

$$a_e = \Gamma_e A_e / dx$$
$$a_w = U_w A_w + \Gamma_w A_w / dx$$
$$a_s = \Gamma_s A_s / dy$$
$$a_n = U_n A_n + \Gamma_n A_n / dy$$
$$a_p = \Gamma_e A_e / dx + U_e A_e + \Gamma_w A_w / dx + \Gamma_n A_n / dy + U_s A_s + \Gamma_s A_s / dy$$

The water continuity equation for the grid cell is:

$$U_e A_e - U_w A_w + U_n A_n - U_s A_s = 0$$

or:

$$U_e A_e + U_n A_n = U_s A_s + U_w A_w$$

If the above equation is inserted into the expression for a_p, the equation

$$a_p = a_e + a_w + a_n + a_s$$

is verified to be correct.

Note that the equations above are only valid if the velocity flows in the same direction as given on the arrows in the figure above.

For a 2D width-averaged sediment calculation in a sand trap, north-south direction is often used as the vertical direction. Further simplifications are:

- uniform the water flow
- negligible horizontal diffusion

Then, the vertical velocity is equal to the sediment particle fall velocity, w. Also, the grid is orthogonal and two-dimensional, so $A_e = A_w = dy$, and $A_n = A_s = dx$. The weighting factors then become:

$a_e = 0.0$

$a_w = U \, dy$

$a_s = \Gamma \, dx \, / \, dy$

$a_n = w \, dx + \Gamma \, dx \, / \, dy$

3.5 The Power-Law Scheme

The Power-Law scheme (POW) is a first-order upstream scheme, where the turbulent term is reduced by multiplying it with a factor *f*. The factor *f* is between 0 and 1.

The formula for f can be derived mathematically by solving the 1D convection-diffusion equation analytically. The factor then becomes:

$$f = \frac{1}{e^{Pe} - 1} \qquad\qquad (3.5.1)$$

where *Pe* is the Pechlet number defined by:

$$Pe = \rho U L / \Gamma \qquad\qquad (3.5.2)$$

L is the length of the cell.

Early computers used relatively long time to calculate the exponential function of Formula 3.5.1. Instead, a power-function was used. This gave name to the Power-Law scheme:

$$f = \max\left[0, \left(1 - \frac{0.1\,|\rho U L|}{\Gamma}\right)^5\right] \qquad\qquad (3.5.3)$$

Convergence of the solution is described in Chapter 3.7. The first-order upstream method and the POW scheme converges relatively easy. A problem with the first order upstream schemes can be large amounts of false diffusion. This is further described in Chapter 3.8. To decrease the amount of false diffusion, while keeping some stability, a second-order upstream method can be used. This is described in the following.

3.6 The Second Order Upstream Scheme

The Second-Order Upstream (SOU) method is based on a second-order accurate method to calculate the concentration on the cell surfaces. The method only involves the convective fluxes, and the diffusive terms are calculated as before. The following figure shows the calculation of the concentration on the west side of cell *p*: side *W*:
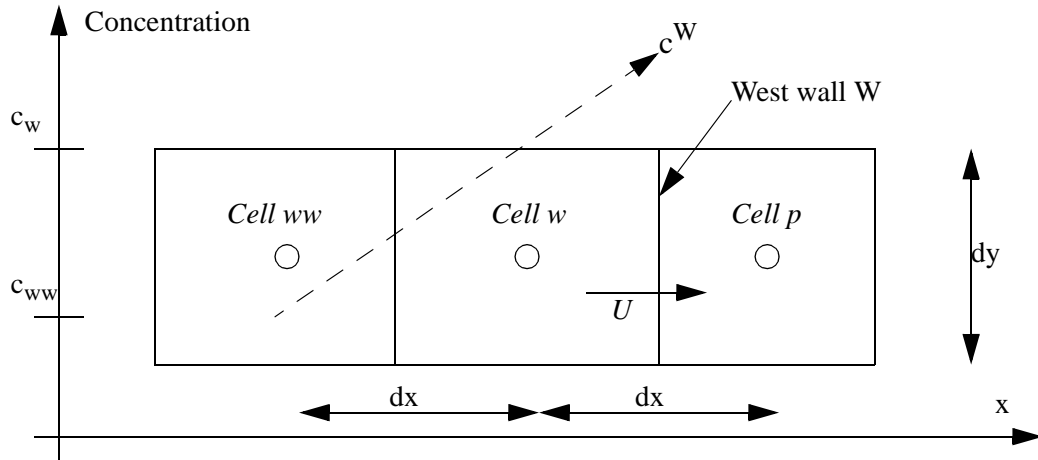
The cell on the west side of cell *w* is called cell *ww*. The concentration in this cell is denoted c_{ww}. The concentration in cell *w* is denoted c_w and the concentration on side *W* of cell *p* is denoted c^W. The SOU scheme uses the concentration in cell *ww* and cell *w* to extrapolate linearly to side *W*. Given the width of the cell in the x-direction is *dx*, and the height in the y-direction is *dy*, it is possible to derive a formula for the concentration on side *W* by triangulation:

$$(c^W - c_{ww}) / (dx + 0.5dx) = (c_w - c_{ww}) / dx$$

or

$$c^W = 3/2\ c_w - \tfrac{1}{2}\ c_{ww} \qquad\qquad (3.6.1)$$

Equation 3.6.1 is only valid if the cells are of equal size. If the expansion ratio is different from unity, a separate formula needs to be applied, where the coefficients 3/2 and ½ are given as a function of the expansion ratio.

The calculation molecule now gets nine cells, as shown in the figure to the right
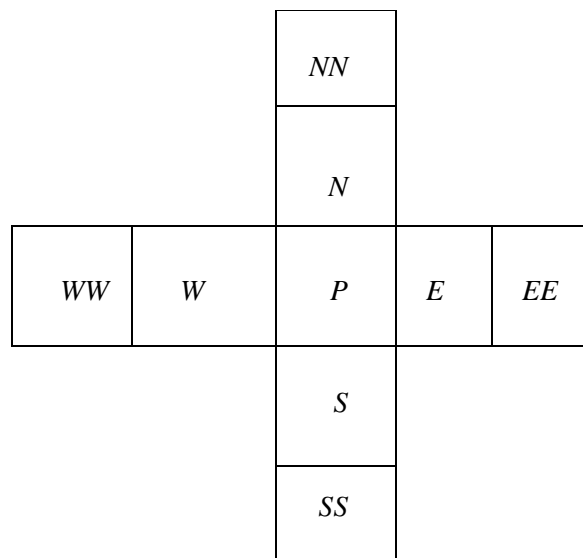
The flux through the west side of cell p then becomes:

West side: $F_w = U_w\ A_w\ (3/2\ c_w - 1/2\ c_{ww}) + \Gamma_w\ A_w\ (c_w - c_p) / dx$

For the other sides, the following fluxes are obtained:

East side: $F_e = U_e A_e (3/2 c_p - 1/2 c_w) + \Gamma_e A_e (c_p - c_e) / dx$

North side: $F_n = U_n A_n (3/2 c_n - 1/2 c_{nn}) + \Gamma_n A_n (c_n - c_p) / dy$

South side: $F_s = U_s A_s (3/2 c_p - 1/2 c_n) + \Gamma_s A_s (c_p - c_s) / dy$

Again, the equations are only valid for uniform water flow. The weighting factors becomes:

$a_e = \Gamma_e A_e / dx$

$a_w = 3/2 U_w A_w + 1/2 U_n A_n + \Gamma_w A_w / dx$

$a_{ww} = - 1/2 U_w A_w$ (3.6.2)

$a_s = \Gamma_s A_s / dy$

$a_n = 3/2 U_n A_n + 1/2 + \Gamma_n A_n / dy$

$a_{nn} = -1/2 U_n A_n$

For the SOU scheme, Equation 3.3.1 now becomes:

$$c_p = \frac{a_w c_w + a_e c_e + a_n c_n + a_s c_s + a_{ww} c_{ww} + a_{nn} c_{nn}}{a_p}$$ (3.6.3)

3.7 The QUICK Scheme

QUICK is an acronym for the Quadratic Upstream Scheme. Instead of using a straight line between cell w and cell ww, a second-order polynomial is used to fit a curve through point ww, w and p. This is further described in the figure below:
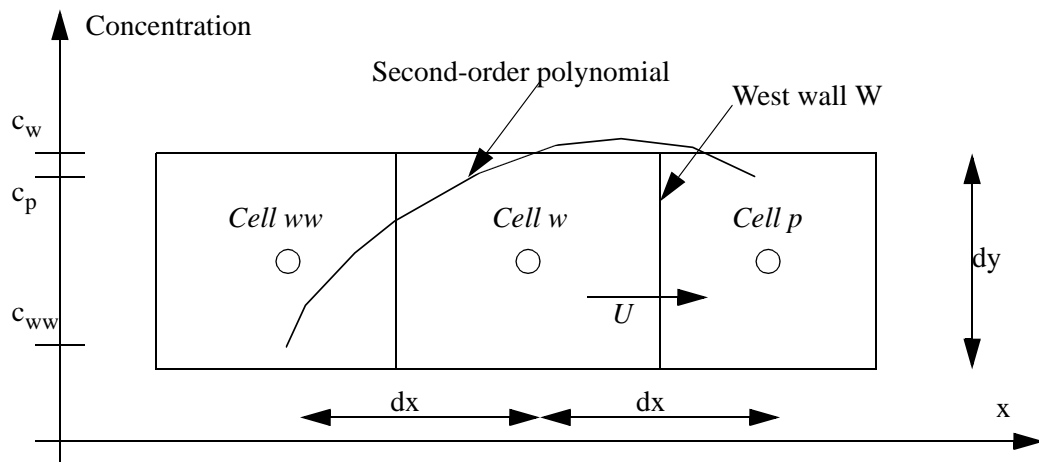
The curve follow the equation

$c = ax^2 + bx + d$ (3.7.1)

With the boundary conditions

23

$c(0) = c_{ww}$

(3.7.2)

$c(1) = c_w$

$c(2) = c_p$

Inserting the boundary conditions of Equation 3.7.2 into Equation 3.7.1, and evaluating the concentration c^W at the wall as $c(1.5)$ gives:

$c^w = 3/8\ c_p + 3/4\ c_w - 1/8\ c_{ww}$

This is then used in the continuity equation as for the other schemes. For example:

West side flux: $F_w = U_w\ A_w\ (3/8\ c_p + 3/4\ c_w - 1/8\ c_{ww}) + \Gamma_w\ A_w\ (c_w - c_p)\ /\ dx$

The remaining derivation of the weighting coefficients is left to the reader.

There exist a large number of other discretization procedures. These differ in the way the concentration on the cell surface is calculated. Extrapolation, interpolation and various number of neighbouring grid cells are used.

3.8 Flux limiter schemes

Some schemes, for example the SOU scheme, have the disadvantage of not being **bounded**. The concentration in a cell may become higher or lower than the concentration in the neighbouring cells. The reason is the negative coefficient for the cells far away (a_{ww} and a_{nn} in Equation 3.6.2). In a scheme with only positive coefficients, the solution is always bounded.

In a not bounded scheme it is possible that negative sediment concentrations occur. This is not physically correct. The main idea of the flux limiter procedure is to limit the concentration on a cell side to stay within certain limits. For example, the concentration on a wall should never be below zero. Another popular criteria is to limit the concentration to the values on the two cells neigbouring the cell surface.

The flux limiter procedure can be applied to both the SOU and the QUICK scheme. Since the POW scheme is always bounded, a flux limiter scheme will have no effect.

A good description of flux limiter schemes is given by Tamamidis and Assanis (1993), including examples with comparisons of different discretization methods with and without flux limiters.

3.9 Simple turbulence models

The turbulence model determines the value of the sediment concentration diffusivity.

The simplest turbulence model is the constant diffusivity model, when the turbulent diffusivity is set constant throughout the computational domain. As an example, a value of 1000 times the kinematic viscosity could be used. The approach is fairly crude, but has nevertheless given reasonable results in some cases.

A better way to find the turbulent diffusivity for rivers is to use the following formula:

$$\Gamma = \alpha \, U_* \, H \qquad\qquad (3.9.1)$$

U_* is the shear velocity and H is the water depth. The parameter α is an empirical constant. A value of 0.11 is often used (Keefer, 1971).

Equation 3.9.1 gives the maximum diffusivity in a vertical profile. Some theoretical solutions give a parabolic shape of the profile, with zero at the water surface and at the bed. However, measurements (Naas, 1977) gave a slightly different profile, as given on the figure on the next page.

Vertical distribution of diffusion
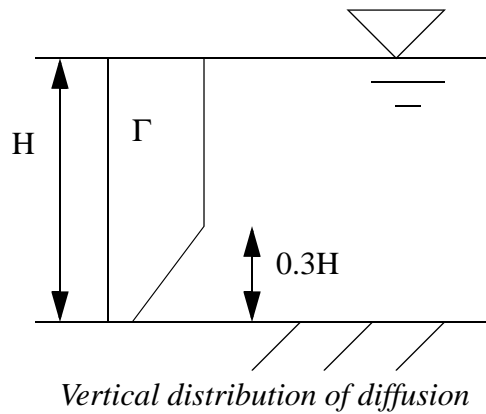
The diffusivity in the cell closest to the bed is given by the following formula:

$$\Gamma_{bed} = 2.4 \, U \, \delta \qquad\qquad (3.9.2)$$

δ is the distance from the bed to the centre of the bed cell. U is the depth-averaged water velocity.

3.10 Boundary conditions

Boundary conditions are required on all boundaries for the sediment flow calculation. The two most used types of boundary conditions are:

• Zero gradient
• Dirichlet

Zero gradient boundary conditions means the derivative of the variable at the boundary is zero. In other words, the value at the boundary is the same as the value in the cell closest to the boundary. For an iterative solution procedure, this is straightforward to program: For each iteration, set the boundary value equal to the value at the cell closest to the boundary. This boundary condition is often used at the outflow boundary for the sediment concentration calculation. It can also be used at walls.

Zero gradient boundary condition is a type of Neumann boundary condition. A Neu-

mann boundary condition is defined as a given gradient prescribed on the boundary.

Dirichlet boundary conditions means the values of a variable is given at the boundary. For example, zero sediment concentration is usually set at the water surface. Also, at the upstream boundary the sediment concentration has to be given.

One of the most challenging problems is the boundary condition for the sediment concentration at the bed. For a general calculation, the sediments should be able to both settle and erode, depending on the shear stress at the bed, the sediment particle size distribution, the in and outflow of sediments from a section and the availability of sediments for erosion. This can be done in two ways:

A. Define a pick-up rate of sediments where erosion occur.
B. Use an equilibrium concentration in the cell close to the bed.

Method B is used in the SSIIM program, so this is further described in the following text. The theory of equilibrium concentration at the bed was first described by Einstein (1950), in his formula for sediment transport. The method has since then been expanded by Toffalletti, and the latest contribution is from van Rijn (1987). Van Rijn made a formula for the equilibrium concentration at the bed:

$$c = 0.015 \frac{d_{50}}{a} \frac{T^{1.5}}{D_*^{0.3}} \qquad (3.10.1)$$

The parameter a is the distance from the concentration point to the bed, the mean sediment particle diameter is denoted d_{50}, $T = (\tau - \tau_c)/\tau$, where τ is the shear stress, τ_c is the critical shear stress for movements of sediment particles, and D_* is given by:

$$D_* = d_{50} \left[\frac{\rho_s - \rho_w}{\rho_w \nu^2} \right]^{\frac{1}{3}} \qquad (3.10.2)$$

Here, ρ_s is the density of the sediment, ρ_w is the density of water and ν is the kinematic viscosity of water.

This formula is used in the cells close to the bed, as a boundary condition at the bed.

3.11 Time-dependent calculations

Time-dependent calculations involves an extra term in the convection-diffusion equations, resulting in:

$$\frac{\partial c}{\partial t} + U_j \frac{\partial c}{\partial x_j} + w \frac{\partial c}{\partial z} = \frac{\partial}{\partial x_j}\left(\Gamma_T \frac{\partial c}{\partial x_j}\right) \qquad (3.11.1)$$

The time term is added as an extra source terms in the discretized equation, integrating over the cells.

The discretization procedure for time-dependent calculation often involves the question of an explicit versus implicit procedure. The following figure explains this, for a one-dimensional time-dependent case. The north-south direction has been replaced by the time dimension.
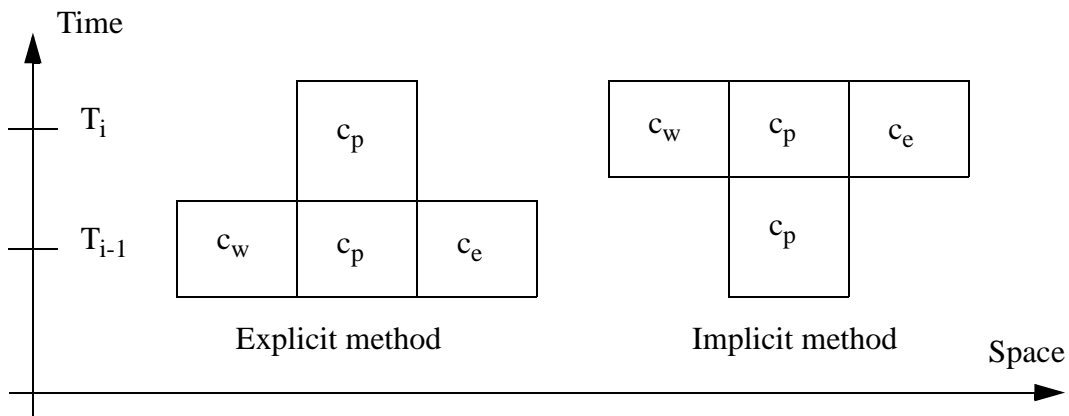
Given the starting values, the question is how to calculate the unknown c_p at time step i as a function of c_p at the previous time step and as a function of the neighbour values c_w and c_e. An explicit method is the easiest, because then the neighbour values are already known. In an implicit method the neighbour values are unknown, and a more complicated solver is needed. The implicit method is, however, more stable than the explicit method.

Also for steady-state solutions, iterations are needed, and the calculation procedure resembles the time-dependent solution. It is also then possible to use implicit or explicit solvers.

3.12 Stability and convergence

The discretization schemes given in Chapter 3.2 are all fairly stable for the calculation of sediment concentration. However, other schemes developed earlier were not so stable. The classical example is the central-difference scheme. In this method, the flux on a cell wall is calculated by interpolation between the cells on the two sides. The figure below shows the estimation.

The flux through side W is then:

West side: $Fw = 0.5\, U_w\, A_w\, (c_w + c_p) + \Gamma_w\, A_w\, (c_w - c_p) / dx$

The same calculation for the other sides gives:

East side: $Fe = 0.5\, U_e\, A_e\, (c_w + c_p) + \Gamma_e\, A_e\, (c_p - c_w) / dx$

North side: $Fn = 0.5\, U_n\, A_n\, (c_n + c_p) + \Gamma_n\, A_n\, (c_n - c_p) / dy$

South side: $Fs = 0.5\, U_s\, A_s\, (c_s + c_p) + \Gamma_s\, A_s\, (c_p - c_s) / dy$

Continuity gives $Fw-Fe+Fn-Fs=0$.

The coefficients become:

$a_e = -0.5\, U_e\, A_e + \Gamma_e\, A_e / dx$

$a_w = 0.5\, U_w\, A_w + \Gamma_w\, A_w / dx$

$a_s = -0.5\, U_s\, A_s + \Gamma_s\, A_s / dy$

$a_n = 0.5\, U_n\, A_n + \Gamma_n\, A_n / dy$

$a_p = -0.5\, U_w\, A_w + \Gamma_w\, A_w / dx + 0.5\, U_e\, A_e + \Gamma_e\, A_e / dx$
$\qquad -0.5\, U_n\, A_n + \Gamma_n\, A_n / dy + 0.5\, U_s\, A_s + \Gamma_s\, A_s / dy$

Applying continuity, the following simplification can be done for a_p:

$a_p = \Gamma_e\, A_e / dx + \Gamma_e\, A_e / dx + \Gamma_n\, A_n / dy + \Gamma_s\, A_s / dy$

Looking at for example a_e, if the diffusivity is low compared with the velocity, there is a chance that a_e can become negative. A negative weighting factor is not physically realistic, and this causes instabilities. The minimum value of the diffusivity before instability occur can be calculated by setting the weighting factor to zero.

$a_e = -0.5\, U_e\, A_e + \Gamma_e\, A_e / dx = 0$

This gives the following minimum viscosity to avoid instabilities:

$\Gamma_{e,min} = 0.5\, U_e\, dx$

28
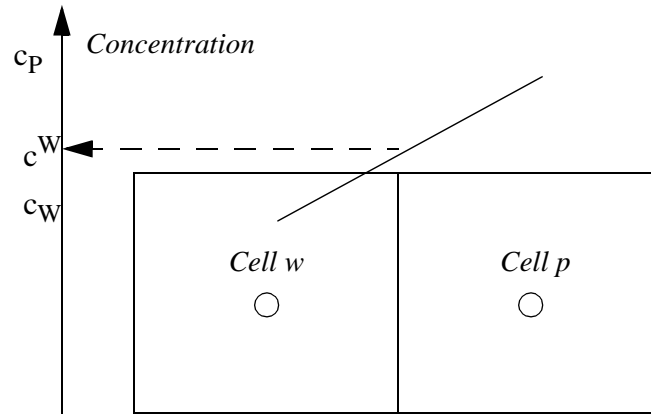
Schemes based on the central-difference scheme or similar ill-formulated numerical schemes will require adding extra diffusivity to the solution in order to become stable. This is called artificial diffusivity, and comes in addition to the physical diffusivity. The disadvantage with adding artificial diffusivity is that the increased diffusivity it may give a different final result than what the natural diffusion would give.

There are usually no problems with convergence for calculation of sediment concentration based on upstream schemes.

3.13 False diffusion

False diffusion is due to the approximations in the convective terms in the discretization schemes. More specifically, how the concentration on the cell side is calculated. The effect is best shown with a coarse grid and steep gradients, for example the following situation:

A sand trap is calculated with 5 x 5 cells in the vertical and horizontal direction, respectively. The cells are 1 meter high and 5 meters long. The water velocity is 0.3 m/s, and the sediment fall velocity is 6 cm/s. The sediments are added from a point source at the water surface, over a length of 5 meters. There is **no** turbulence! This gives the following theoretical concentration profile in the flow:
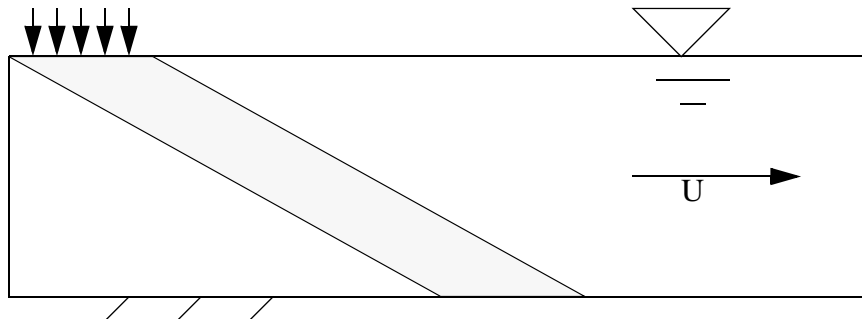
The concentration is unity along a band in the flow. The concentration is zero elsewhere.

The first-order upstream scheme is used to calculate the concentration. The following coefficients are obtained:

$a_t = 0.06 * 5 = 0.3$
$a_w = 0.3 * 1 = 0.3$
$a_b = 0.0$
$a_e = 0.0$
$a_p = 0.6$

This gives $a_t/a_p = 0.5$ and $a_w/a_p = 0.5$. In other words, the concentration in a cell is the

average of the concentration in the cell above and in the cell upstream. The boundary condition is a concentration of unity in one cell at the surface, and zero concentration in the other surface cells and the inflow cells. The following result is obtained:

0.5	0.25	0.125	0.0625	0.0313	0.0156
0.25	0.25	0.188	0.125	0.0781	0.0469
0.125	0.188	0.188	0.156	0.117	0.0820
0.0625	0.125	0.156	0.156	0.137	0.109
0.0313	0.0781	0.117	0.137	0.137	0.123

Grid with concentration values

The maximum concentration has decreased from unity to 0.137 at the bed. It has also been smeared out over several cells at the bed.

False diffusion can be avoided by:

- using higher order schemes
- aligning the grid with the flow direction
- increasing the number of grid cells

3.14 Spreadsheet programming

Given the water flow field, it is possible to make a spreadsheet for calculation of the sediment concentration. One application is to calculate the trap efficiency of a sand trap. Then a two-dimensional width-averaged approach is used. A structured orthogonal grid is used, where each cell in the grid is simulated by a cell in the spreadsheet. If a uniform water velocity and turbulence field can be assumed in the vertical direction, then the same a_{nb} coefficients can be used for all the cells. A more advanced approach is to use a logarithmic velocity distribution, and a given distribution of the eddy-viscosity.

If the simpler approach is used, the coefficients a_{nb} can be calculated before the programming starts. This is based on the formulas given previously, and a chosen number of grid cells. The grid is structured, orthogonal and all cells have the same size.

A figure of this spreadsheet is given below, with 9 cells in the vertical direction, and 12 cells in the horizontal direction. The size of the grid can of course be changed according to the dimensions of each problem.

Table 1: Spreadsheet programming

	A	B	C	D	E	F	G	H	I	J	K
1		0	0	0	0	0	0	0	0	0	0
2	X										Y
3	X										Y
4	X										Y
5	X										Y
6	X										Y
7	X										Y
8	X										Y
9	X										Y
10	X	Z	Z	Z	Z	Z	Z	Z	Z	Z	Y

The cells marked X are inflow boundary conditions. These are the A2..A10 cells. A concentration value is given in these cells. A constant value can be given, or it is possible to use a formula for the vertical distribution of the concentration.

The cells marked 0 is the boundary condition at the water surface. This is zero.

The cells marked Y is the outflow boundary condition. If the horizontal diffusion is assumed to be zero, the values in these cells will not affect the computation. If the horizontal diffusion is non-zero, a zero gradient boundary condition can be used. Then the formula in these cells should be:

Cell K2: +J2
Cell K3: +J3
 ...
Cell K10: +J10

The cells marked Z is the bed boundary condition. A formula for the equilibrium sediment concentration can be used, for example van Rijn's formula. However, often the shear stress is below critical at the bed of the sand trap, giving zero concentration. This will not be correct, as the sediment concentration at the bed will always be higher than the cell above. Therefore, the concentration can be set equal to the concentration in the cell above.

(Note that a more detailed calculation will give a very low diffusion coefficient close to the bed of the sand trap, meaning the concentration in the cell above the bed is independent of the concentration in the bed boundary. For a simplified calculation, the dif-

fusion coefficient is significant. Then the same result is obtained if zero gradient boundary condition is used.)

Cell B10: +B9
Cell C10: +C9
...
Cell J10: + J9

The discretized formula now has to be given in all the remaining interior cells. As an example, the following data is assumed:

$a_w = 0.1$
$a_t = 0.2$
$a_s = 0.006$
$a_b = 0.002$
$a_p = 0.308$

Starting in cell B2, we give the following formula:

+(0.1*a2+0.2*b1+0.006*c2+0.002*b3)/0.308

This formula is copied to all the interior cells, from cell B2 to J9. Afterwards, the calculation has to be repeated some times to get convergence. The repetition is dependent on the particular spreadsheet program. For Lotus 123, use *F9* on the keyboard repeatedly. For MS Excel, use the menu *Tools, Options, Calculations*, and cross off *Iterations*, and give a number in the edit-field, for example 50.

The trap efficiency is calculated by first summing the inflow and the outflow:

Inflow: sum of cells A2..A10
Outflow: sum of cells K2..K10

Trap efficiency = (Inflow-Outflow)/Inflow

3.15 Exercises

Problem 3.1

Determine the sediment trap efficiency in a desilting basin, 60 m long, 4 m wide and 3 m deep. The water inflow is 3 m^3/s, and the sediment particles have a diameter of 0.2 mm.

Use a two-dimensional numerical model with a first-order upstream scheme, and a minimum of 200 cells. Neglect entrance effects and assume uniform flow. Also assume constant vertical distribution of velocity and eddy-viscosity. Assume constant

vertical sediment concentration distribution at the inflow boundary. The temperature is 20 degrees Centigrade. A Manning's value of n=0.013 can be assumed.

Problem 3.2

Do the same calculation as problem 1, but use four times as many grid cells. What is the trap efficiency? Why does it change compared with the result from Problem 1?

Problem 3.3

Do the same calculation as problem 1, but use the SOU scheme instead. What is the trap efficiency? Why does it change compared with the result from Problem 1?

Problem 3.4

Expand problem 1, taking into account the vertical distribution of velocity and sediment diffusivity. What is the change in trap efficiency? What are the main physical reasons for the change?

Problem 3.5

Derive the weighting coefficient for the Central-difference scheme in detail.

Problem 3.6

Carry out the detailed derivation of the weighting coefficient for the SOU scheme. Can negative coefficients occur? Will this lead to stability problems?

4. Calculation of water velocity

This chapter describes the solution procedures for the Navier-Stokes equations. These equations describe the water velocity and turbulence in a river or a hydraulic system.

4.1 The Navier-Stokes equations

The Navier-Stokes equations describe the water velocity. The equations are derived on the basis of equilibrium of forces on a small volume of water in laminar flow. For turbulent flow, it is common to use the Reynolds' averaged versions of the equations. The Reynolds' averaging is described first.

We are looking at a time series of the velocity at a given location in turbulent flow:
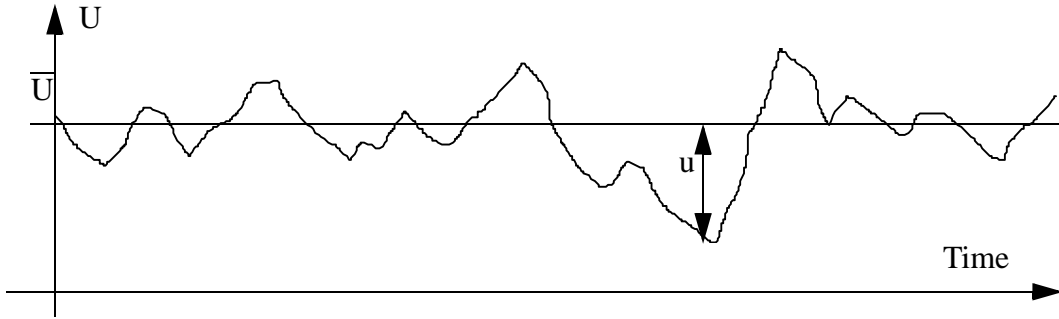
The velocity is divided into an average value U, and a fluctuating value u. The two variables are inserted into the Navier-Stokes equation for laminar flow, and after some manipulations and simplification the Navier-Stokes equation for turbulent flow emerges:

$$\frac{\partial U_i}{\partial t} + U_j \frac{\partial U_i}{\partial x_j} = \frac{1}{\rho} \frac{\partial}{\partial_j} (-P\delta_{ij} - \rho \overline{u_i u_j}) \qquad (4.1.1))$$

P is the pressure and δ_{ij} is the Kronecker delta, which is 1 if i=j and 0 if i≠ j. The last term is the Reynolds stress term, often modelled with the Boussinesq' approximation:

$$-\rho \overline{u_i u_j} = \rho \nu_T \left(\frac{\partial U_i}{\partial x_j} + \frac{\partial U_j}{\partial x_i} \right) - \frac{2}{3} \rho k \delta_{ij} \qquad (4.1.2)$$

The variable k is the turbulent kinetic energy. This is further described in Chapter 4.3. Inserting Equation 4.1.2 into Equation 4.1.1 and regrouping the variables:

$$\frac{\partial U_i}{\partial t} + U_j \frac{\partial U_i}{\partial x_j} = \frac{1}{\rho} \frac{\partial}{\partial x_j} \left[-\left(P + \frac{2}{3}k \right) \delta_{ij} + \nu_T \frac{\partial U_i}{\partial x_j} + \nu_T \frac{\partial U_j}{\partial x_i} \right] \qquad (4.1.3)$$

There are basically five terms: a transient term and a convective term on the left side of

the equation. On the right side of the equation there is a pressure/kinetic energy term, a diffusive term and a stress term. Important note:

The convective and diffusive term are solved with the same methods as the solution of the convection-diffusion equation for sediment transport. The difference is that the sediment concentration is replaced by the velocity.

The stress term is sometimes neglected, as it has very little influence on the solution for many cases. The pressure/kinetic energy term is solved as a pressure term. The kinetic energy is usually very small, and often negligible compared with the pressure.

A difference between Equation 4.1.3 and the convection-diffusion equation for sediments is the diffusion coefficient. Equation 4.1.3 includes an eddy-viscosity instead of the diffusion coefficient. The relationship between these two variables is:

$$\nu_T = Sc \; \Gamma \qquad\qquad (4.1.4)$$

where Sc is the Schmidt number. This is usually set to unity, meaning *the eddy-viscosity is the same as the turbulent sediment diffusivity.*

This leaves the problem of solving the pressure term. Several methods exist, but with the control volume approach, the most commonly used method is the SIMPLE method. This is described in the next chapter.

4.2 The SIMPLE method

SIMPLE is an abbreviation for Semi-Implicit Method for Pressure-Linked Equations. The purpose of the method is to find the unknown pressure field. The main idea is to guess a value for the pressure and use the continuity defect to obtain an equation for a pressure-correction. When the pressure-correction is added to the pressure, water continuity is satisfied.

To derive the equations for the pressure-correction, a special notation is used. The initially calculated variables do not satisfy continuity and are denoted with an index *. The correction of the variables is denoted with an index '. The variables after correction do not have a superscript. The process can then be written:

$$P = P^* + P' \qquad\qquad (4.2.1)$$
$$U_k = U_k^* + U_k' \qquad\qquad (4.2.2)$$

P is the pressure and *U* is the velocity. The index *k* on the velocity denotes direction, and runs from 1 to 3 for a 3D calculation.

Given guessed values for the pressure, the discretized version of the Navier-Stokes equations is:

$$a_p U^*{}_p \;=\; \sum_{nb} a_{nb} U^*{}_{nb} + B_{u_k} - \left(A_k^j \frac{\partial P^*}{\partial \xi} \right) \qquad (4.2.3)$$

The convective and diffusive terms have been discretized as described in Chapter 3. The variable *B* contains the rest of the terms besides the convective term, the diffusive term and the pressure term. In the pressure term, *A* is the surface area on the cell wall, and ξ is an index for the non-orthogonal coordinate system, described in Chapter 2.1.

The discretized version of the Navier-Stokes equations based on the corrected variables can be written as:

$$a_p U_p \;=\; \sum_{nb} a_{nb} U_{nb} + B_{u_k} - \left(A_k^j \frac{\partial P}{\partial \xi} \right) \qquad (4.2.4)$$

If this equation is subtracted from Equation 4.2.3, and the two Equations 4.2.2 and 4.2.3 are used, the following equation emerges for the velocity correction:

$$U_{k_p}{}' \;=\; \left(\frac{A_k^j}{\left(a_p - \sum_{nb} a_{nb} \right)} \frac{\partial P'}{\partial \xi^j} \right) \qquad (4.2.5)$$

The SIMPLEC method uses the formula above. The SIMPLE method omits one term in the above equation:

$$U_{k_p}{}' \;=\; \left(\frac{A_k^j}{a_p} \frac{\partial P'}{\partial \xi^j} \right) \qquad (4.2.6)$$

The above equations give the velocity-corrections once the pressure-corrections are known. To obtain the pressure-corrections, the continuity equation is used for the velocity correction for a cell:

$$\sum_{nb} A_k U'_k \;=\; 0 \qquad\qquad (k=1,2,3) \qquad (4.2.7)$$

Equation 4.2.6 is inserted into Equation 4.2.7. The result is an equation of the following form:

$$a_p P'_p \;=\; \sum_{nb} a_{nb} P'_{nb} + b \qquad (4.2.8)$$

The source term, *b*, in Equation 4.2.8 turns out to be the water continuity defect. The equation is solved in the same way as the other equations.

The procedure is therefore:

1. Guess a pressure field, *P**
2. Calculate the velocity *U** by solving Equation 4.2.3
3. Solve equation 4.2.8 and obtain the pressure-correction, *P'*
4. Correct the pressure by adding *P'* to *P**
5. Correct the velocities *U** with *U'* using equation 4.2.6.
6. Iterate from point 2 to convergence

An equation for the pressure is not solved directly, only an equation for the pressure-*correction.* The pressure is obtained by accumulative addition of the pressure-correction values.

The SIMPLE method can give instabilities when calculating the pressure field. Therefore, the pressure-correction is often multiplied with a number below unity before being added to the pressure. The number is a relaxation coefficient. The value 0.2 is often used. The optimum factor depend on the flow situation and can be changed to give better convergence rates. Relaxation coefficients are further described in Chapter 4.5.

Regarding the difference between the SIMPLE and the SIMPLEC method, the SIMPLEC should be more consistent in theory, as a more correct formula is used. Looking at Equations 4.2.5 and 4.2.6, the SIMPLE method will give a lower correction than the SIMPLEC method, as the denominator will be larger. The SIMPLE method will therefore move slower towards convergence than the SIMPLEC method. If there are problems with instabilities, this can be an advantage.

A more detailed description of the SIMPLE method is given by Patankar (1980).

4.3 Advanced turbulence models

The following chapter is a rather brief overview of advanced turbulence models. The reader is referred to White (1974) and Rodi (1980) for more detailed description of turbulence and turbulence models.

In chapter 4.1, the Boussinesq approximation was introduced for finding an expression for the Reynolds' stress term:

$$-\rho \overline{u_i u_j} \;=\; \rho \nu_T \left(\frac{\partial U_i}{\partial x_j} + \frac{\partial U_j}{\partial x_i} \right) - \frac{2}{3} \rho k \delta_{ij} \qquad (4.3.1)$$

ν_T is the turbulent eddy viscosity.

Note:

The kinematic viscosity is a fluid property, while the turbulent eddy-viscosity depends of the velocity field.

Some simpler turbulence models were described in Chapter 3. These models require calibration before being used on new cases.

The k-ε model

The k-e model models the eddy-viscosity as:

$$\nu_T = c_\mu \frac{k}{\varepsilon^2} \tag{4.3.2}$$

k is turbulent kinetic energy, defined by:

$$k \equiv \frac{1}{2}\overline{u_i u_i} \tag{4.3.3}$$

k is modelled as:

$$\frac{\partial k}{\partial t} + U_j \frac{\partial k}{\partial x_j} = \frac{\partial}{\partial x_j}\left(\frac{\nu_T}{\sigma_k}\frac{\partial k}{\partial x_j}\right) + P_k - \varepsilon \tag{4.3.4}$$

where P_k is given by:

$$P_k = \nu_T \frac{\partial U_j}{\partial x_i}\left(\frac{\partial U_j}{\partial x_i} + \frac{\partial U_i}{\partial x_j}\right) \tag{4.3.5}$$

The dissipation of k is denoted ε, and modelled as:

$$\frac{\partial \varepsilon}{\partial t} + U_j \frac{\partial \varepsilon}{\partial x_j} = \frac{\partial}{\partial x_j}\left(\frac{\nu_T}{\sigma_k}\frac{\partial \varepsilon}{\partial x_j}\right) + C_{\varepsilon 1}\frac{\varepsilon}{k}P_k + C_{\varepsilon 2}\frac{\varepsilon^2}{k} \tag{4.3.6}$$

The constants in the *k*-ε model have the following standard values:

$$
\begin{aligned}
c_\mu &= 0.09 \\
C_{\varepsilon 1} &= 1.44 \\
C_{\varepsilon 2} &= 1.92 \\
\sigma_k &= 1.0 \\
\sigma_\varepsilon &= 1.3
\end{aligned}
\tag{4.3.7}
$$

The main advantage of the *k*-ε model is the almost universal constants. The model can thereby be used on a number of various flow situations without calibration. For river engineering this may not always be the case, because when friction along the bed is influencing the flow field, the roughness of the bed also needs to be given. If the roughness can not be obtained from direct measurements, it has to be calibrated with measurements of the velocity.

As seen from Equation 4.3.1, the eddy-viscosity is isotropic, and modelled as an average for all three directions. Schall (1977) investigated the eddy-viscosity in a laboratory flume in three directions. His work shows that the eddy-viscosity in the streamwise direction is almost one magnitude greater than in the cross-streamwise direction. A better turbulence model could therefore give more accurate results for many cases.

More advanced turbulence models

To be able to model non-isotropic turbulence, a more accurate representation of the Reynolds stress is needed. Instead of using the Boussinesq approximation (Equation 4.3.1), the Reynolds' stress can be modelled with all terms:

$$-\rho \overline{u_i u_j} = -\rho \begin{bmatrix} \overline{uu} & \overline{vu} & \overline{vu} \\ \overline{uv} & \overline{vv} & \overline{wv} \\ \overline{uw} & \overline{vw} & \overline{ww} \end{bmatrix} \tag{4.3.8}$$

The following notation is used: *u* is the fluctuating velocity in direction 1, *v* is the fluctuating velocity in direction 2 and *w* is the fluctuating velocity in direction 3.

The nine terms shown on the right hand side of Equation 4.3.8 can be condensed into six different terms, as the matrix is symmetrical. A Reynolds' stress model will solve an equation for each of the six unknown terms. Usually, differential equations for each term are solved. This means that six differential equations are solved compared with two for the *k*-ε model. It means added complexity and computational time.

An alternative is to use an Algebraic Stress Model (ASM), where algebraic expressions for the various terms are used. It is also possible to combine the *k*-ε model with an ASM to obtain non-isotropic eddy viscosity (Rodi, 1980).

An even more advanced method is to resolve the larger eddies with a very fine grid, and use a turbulence model only for the smaller scales. This is called Large-Eddy Simulation (LES). If the grid is so fine that sub-grid eddies do not exist because they are dissipated by the kinematic viscosity, the method is called a Direct Solution (DS) of the Navier-Stokes equations.

Note that both LES and especially DS modelling require extreme computational

resources, which presently is not feasible for engineering purposes.

4.4 Boundary conditions

Boundary conditions for the Navier-Stokes equations are in many ways similar to the solution of the convection-diffusion equation. In the following text, a division in four parts is made: Inflow, outflow, water surface and bed/wall.

Inflow

Dirichlet boundary conditions have to be given at the inflow boundary. This is relatively straightforward for the velocities. Usually it is more difficult to specify the turbulence. It is then possible to use a simple turbulence model, like Equation 3.4.1 to specify the eddy-viscosity. Given the velocity, it is also possible to estimate the shear stress at the entrance bed. Then the turbulent kinetic energy k at the inflow bed is determined by the following equation:

$$k = \frac{\tau}{\rho\sqrt{c_\mu}} \qquad\qquad (4.4.1)$$

This equation is based on equilibrium between production and dissipation of turbulence at the bed cell.

Given the eddy-viscosity and k at the bed, Equation 4.3.2 gives the value of ε at the bed. If k is assumed to vary linearly from the bed to the surface, with for example half the bed value at the surface, Equation 4.3.2 can be used together with the profile of the eddy-viscosity to calculate the vertical distribution of ε.

Outflow

Zero gradient boundary conditions can be used at outflow boundaries for all variables.

Water surface

Zero gradient boundary conditions are used for ε. The turbulent kinetic energy, k, is set to zero. Symmetrical boundary conditions are used for the water velocity, meaning zero gradient boundary conditions are used for the velocities in the horizontal directions. The velocity in the vertical direction is calculated from the criteria of zero water flux across the water surface.

Bed/wall

The flux through the bed/wall is zero, so no boundary conditions are given. However, the flow gradient towards the wall is very steep, and it would require a significant

number of grid cells to dissolve the gradient sufficiently. Instead, a wall law is used, transformed by integrating it over the cell closest to the bed. Using a wall law for rough boundaries (Schlichting, 1980)

$$\frac{U}{u_*} = \frac{1}{\kappa} \ln \left(\frac{30y}{k_s} \right)$$ (4.4.2)

also takes the effect of the roughness, k_s, on the wall into account. The velocity is denoted U, u_* is the shear velocity, κ is a coefficient equal to 0.4 and y is the distance from the wall to the centre of the cell.

The wall law is used both for the velocities and the turbulence parameters. This is described in more detail by Rodi (1980).

4.5 Stability and convergence

It is generally much more difficult to obtain a stable solution for the water flow calculation than for the sediment calculation.

A number of factors are important to get the solution to converge. The upstream methods and implicit solvers described in Chapter 3 are important. Additionally, some other numerical methods to improve convergence are described in the following.

Relaxation

The main principle in the solution of the equations are to obtain an improvement of a guessed velocity field. Starting with the guessed values, several iterations are done to improve the result. For each iteration, a new guess is made. Let us say that we have finished iteration i-1 and i, and we are looking at what variables, v, we should use when starting iteration i+1. An obvious choice is of course the variables at iteration i. However, introducing the relaxation coefficient, r, instead we use:

$$v = r * v_i + (1-r) * v_{i-1}$$ (4.5.1)

The relaxation coefficients should normally be between 0 and 1.

Relaxation will give a slower convergence speed towards the final solution, but there will be less instabilities. If the solution diverges or does not converge because of instabilities, a normal measure is to lower the relaxation coefficients.

Multigrid and block-correction

The purpose of the multigrid methods is to speed up the convergence of the solution. The main principle is a division of the grid several coarser sub-grids. This is shown in

the figure below:

Coarse grid   *Fine grid*
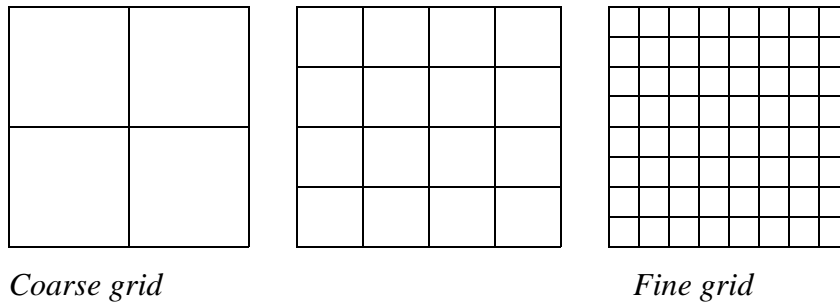
The solution is first iterated once on the coarse grid. It is then extrapolated to the finer grid, where it is iterated further. Then it is extrapolated to the finest grid, where more iterations are done. The solution is interpolated to the medium fine grid, where more iterations are done. Then this is interpolated to the coarse grid, and computed again with more iterations. The sequence is repeated until convergence. There are transformation functions moving the variables from one grid to the other by extrapolation/interpolation. When the finest grid has a high amount of cells, it is possible to have several grids with varying number of grid cells.

A version of the multigrid method is called **block-correction**. For a two-dimensional situation, the grids then look like this:

Original grid   *Coarse grid I*   *Coarse grid II*
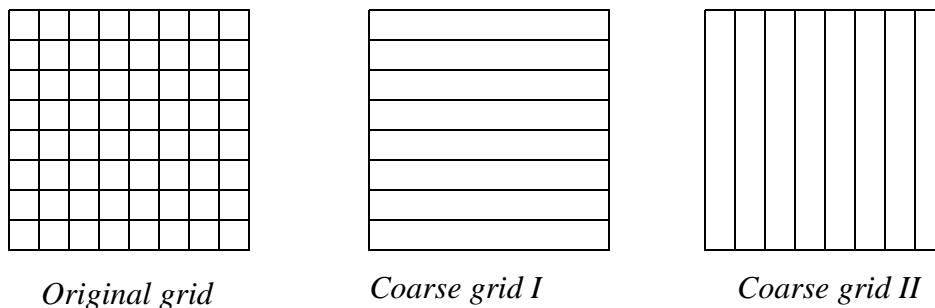
The iterations are started on the original grid. Then all variables are summed in a slice of the grid, so that a one-dimensional grid emerges. This is solved, and the result is used to correct the original values. This is repeated in all directions, shown here with two coarse grids, for a two-dimensional situation.

The Rhie and Chow interpolation

Using a non-staggered (Chapter 2.1) variable location, all variables are calculated in the centre of the cells. This causes oscillations in the solution and instabilities. The staggered grid was invented to avoid these oscillations. Then the pressure is calculated between the centres of the grid cells. There are several problems with this variable arrangement, especially for non-orthogonal grids. The Rhie and Chow interpolation

was invented to avoid the instabilities and still use a non-staggered grid. The interpolation gives the velocity on the cell surface. This velocity is used to calculate the flux on the cell surface.

A derivation of the Rhie and Chow interpolation procedure is quite involved, and the reader is referred to Rhie and Chow (1983). The main idea is to use information about pressure gradients in staggered and non-staggered positions. The resulting interpolation formula is a function of the linearly interpolated velocity plus a term dependent on the pressure gradients, cell areas and the a_p coefficient.

The Rhie and Chow interpolation can be interpreted as an addition of 4th order artificial diffusion.

The Rhie and Chow interpolation is used in most CFD programs using the finite volume method, the SIMPLE algorithm and non-staggered grids.

Note that the Rhie and Chow interpolation has given problems for some cases where there are large source terms in the Navier-Stokes equations (Olsen and Kjellesvig, 1998b). In these cases there are significant forces on the water in addition to the pressure, for example from gravity.

4.6 Exercises

Problem 4.1:

Apply the SSIIM model to the example with the sand trap: Tutorial 1 in the User's Manual. Note how many iterations are required for convergence of the Navier-Stokes equations, and how long time it takes on your PC.

Problem 4.2:

Repeat the calculation in Problem 1, but this time use block-correction for all equations. How many iterations are now needed, and how long time does this take?

Problem 4.3:

Repeat the calculation as in Problem 1, but this time change the relaxation factors first to 1.0 for all the equations. How many iterations are needed?

Again, change the relaxation coefficients to 0.5 for all equations. How many iterations are needed?

Change the relaxation coefficients to 0.3 for velocity, 0.1 for pressure and 0.2 for k and ε. How many iterations are needed?

Problem 4.4:

Repeat the calculation in Problem 1, but this time reduce the influence of the Rhie and Chow interpolation by the using the F 21 data set. Set this to 0.5 for one run and 0.0 for the next run. How does the Rhie and Chow interpolation affect the resulting trap efficiency? And how many iterations are needed?

Problem 4.5:

Repeat the calculation in Problem 1, but this time use uniform upstream and downstream velocity profile. This is done by using the G 7 data sets. How does this affect the convergence rate and the resulting trap efficiency? What are the reasons for the change?

Problem 4.6:

Repeat the calculation in Problem 1 twice, using a roughness of 2 cm and 0.1 mm. This is done by giving the roughness in the F 16 data set. How does the roughness affect the trap efficiency and calculation time? What is the reason for the change?

Problem 4.7:

Calculate the water flow for the fish farm tank example with SSIIM. How many iterations are needed? Remove the G 8 data set with initial velocities in the control file. What happens in the calculations and why? How is it possible to make the calculations converge without lowering the initial water velocities?

5. Short review of the finite element method

In the previous chapters, the finite volume method has been described. Many CFD programs use the finite element method instead. The finite element method is more mathematically oriented, and more difficult to explain by physical processes. A short review is given, where some of the characteristic expressions are described. For a more detailed review, several books can be consulted, for example Taylor and Huges (1981).

The calculation points, or nodes, on a finite element can look like the figure on the right for an element with nine nodes:

Elements can also have for example four nodes, with nodes in the corners only.

The variation of a variable, ϕ, on an element surface is given by the following formula:
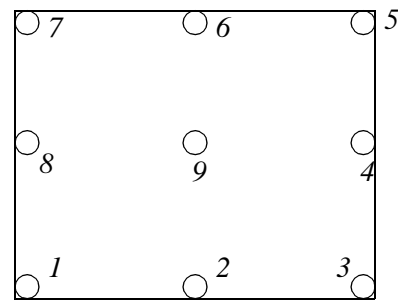

Calculation points in a finite element

$$\phi = \sum_{i=1}^{m} S_i \phi_i \qquad (5.1)$$

The sum is over all the *m* nodes of the element, for example four or nine. The variable S is an **interpolation function**, and it is the same for all the elements. The interpolation function is a polynomial, and a function of the node location on the element. S becomes an array with four or nine elements, depending on how many nodes there are on the element.

The interpolation function describes the variation of a variable over the surface of the cell. If the chosen function is a constant, we get the same distribution as used in the finite volume method.

The finite element method can be formulated in different ways. Often a **weighed residual method** is used. Then the basic equations are multiplied with a **weighting function**, W, and integrated over the element. A **Galerkin formulation** is used if the weighting functions are equal to the interpolation functions (S=W). The result of the integration is a residual, which is minimized. The equation with the residual is called the **residual equation**.

A term often encountered in the finite element method is the **weak formulation**. This means that when formulating the equation system, there are no restrictions that the derivative of the unknown need to exist on the surface between elements, as opposed to the original differential equations. The Galerkin formulation is a weak formulation. The main effect of the weak formulation is that mass continuity need not be satisfied

automatically in the solution procedure.

After integration over an element, there will be one equation with nine/four unknown for each element. For all the n elements in the grid there will be n number of equations and unknowns. Note that almost all the variables are given on the border of a cell, meaning the variable in a point is used in more than one equation. The system of unknown and equations can be set up in a matrix A of unknown coefficients, multiplied with a matrix B with the variable and the result set to zero. The size of A is nxn, and the size of B is 1xn.

A finite element method often uses an unstructured mesh. This means that the matrix A is sparse. To solve the system of equations, the matrix needs to be inverted. This is a fairly time-consuming procedure. A good solver is therefore essential in the finite element method.

Using the finite volume method with a structured grid, there will be a banded structure in matrix A, and also fewer non-zero elements for each row. This means in principle less storage requirement and a much simpler solver.

Also note that the finite element method will give similar problems with stability as the finite volume method. Implicit solvers, high-order upstream schemes etc. is more difficult to formulate with the finite element method than the finite volume method. This especially applies to an unstructured grid, where it is difficult to derive an implicit high-order upstream procedure.

Many finite element programs have employed various techniques to try to overcome these problems, with varying degree of success. The debate of which method is better, the finite volume method or the finite element method, is presently still ongoing. However, almost all commercial general-purpose 3D CFD models uses the finite volume method.

6. Short review of advanced CFD programs for hydraulic engineering

The evolution of CFD programs is progressing very rapidly. The following review is based on experiences from 1990-1999 and information from literature and the Internet. This information will change rapidly as programs evolve and new programs emerge.

The presentation includes both 2D and 3D models. Some of the models are also quasi-3D. This means that hydrostatic pressure is assumed, the models should not be used for bed slopes over 1:10 in the flow direction.

Simpler CFD programs are omitted, and only more advanced models are presented, starting from 2D models with non-orthogonal grids to 3D models. Also, some advanced CFD programs have been omitted as they are not available to the public, and are therefore of less interest. Models used mostly for the marine environment and hydraulic machinery are also omitted.

The price of a program can be related to the cost of a computer. In the price range used in the following text, a relatively inexpensive program is priced in the same range as a PC, and a relatively expensive program is priced in the same range as a high-end UNIX workstation.

6.1 SSIIM

SSIIM is an abbreviation of Sediment Simulation In Intakes with Multiblock option. The program is made for use in hydraulic and sedimentation engineering. It is based on the control volume approach with a 3D structured non-orthogonal grid. The Navier-Stokes equations are solved, and also the convection-diffusion equation for sediment transport.

SSIIM has been used in a number of studies relating to water flow and sediment transport in river and hydropower engineering. This includes trap efficiency of sand traps and hydropower reservoirs, turbidity currents, erosion and local scour, flood waves, head loss and spillways.

More information about SSIIM is available on the WWW pages:

http://www.sintef.no/nhl/vass/vassdrag.html

SSIIM runs only on PC's and it is freeware.

6.2 FLUENT

FLUENT is a general purpose finite volume program made by Fluent Inc. The original program was based on a 3D structured non-orthogonal grid, but the most recent version also has unstructured 3D grids.

Fluent has been used for head loss in a hydropower tunnel gate plug (Olsen and Oldervik, 1995).

More information about FLUENT can be found on the WWW page:

http://www.fluent.com

FLUENT runs on UNIX workstations and it is relatively expensive.

6.3 FIDAP

FIDAP is a general purpose 3D finite element program, currently owned by Fluent Inc. It was originally made for structure analysis, but it has been expanded to flow modelling. The program can use both structured and non-structured grids.

FIDAP has been used for modelling release of water from a hydropower plant to the sea and head loss in a hydropower tunnel gate plug (Olsen and Oldervik, 1995).

More information about FIDAP is available on the WWW page:

http://www.fluent.com/

FIDAP runs on UNIX workstations and it is relatively expensive.

6.4 STAR-CD

STAR-CD is a general-purpose 3D commercial program made by Computational Dynamics Inc. It can use both structured and unstructured grids, with combinations of tetrahedral and hexahedral cells. The grid can be non-orthogonal and nested grids can be used. Of special interest in hydraulic engineering is its ability to model cavitation.

STAR-CD has been used to calculate the coefficient of discharge for a spillway (Yang, 1998).

More information about STAR-CD is given on the WWW page:

http://www.cd.co.uk

STAR-CD runs on both Windows NT on a PC and on UNIX workstations. It is rela-

tively expensive for a commercial license, but less expensive for an academic user.

6.5 TELEMAC

TELEMAC is a finite element program made by for both 2D and quasi 3D flow in hydraulic engineering. It is made by Laboratorie National de Hydraulique in France. The hydrostatic pressure assumption is used for the 3D calculations.

TELEMAC has been used in a number of studies of rivers. It has also been used for calculating the flood wave from the Malpasset dam break, with good comparisons with observed values (Hervouet et. al., 1993).

More information about TELEMAC is given on the web page:

http://www.hrwallingford.co.uk/software/telemac

TELEMAC runs on UNIX workstations and it is relatively expensive. Academic institutions may get a significantly reduced price.

6.6 FLOW-3D

FLOW-3D is a general-purpose finite volume program made by Flow Science Inc. The program is using a 3D **orthogonal** grid. There are several options and possibilities to block out cells or parts of cells. The program has a very good multiphase option, making it particularly well suited for calculation of time-dependent flow with free surface. Flow in a Parshall flume, including a good estimation of the water surface was first calculated using FLOW-3D. See the WWW page:

http://ogee.do.usbr.gov/wc/wm/numerical.html

The program has also been used for calculation of spillways, flood waves from dam breaks and hydraulic jumps (Richardson, 1997).

More information about FLOW-3D is given on the WWW page:

http://www.flow3d.com/

FLOW-3D runs on UNIX workstations and it is relatively expensive.

6.7 TABS

The TABS models are made by Waterways Experiment Station, US Army Corps of Engineers. The purpose of the program is river and hydraulic engineering calculations. The TABS model exist in several forms. The original was TABS-2D, a two-dimen-

sional depth-averaged finite element program, using triangular cells. There is also a quasi-3D version, TABS-3D, also based on the finite element method.

The TABS models have been used in a large number of river engineering studies, for example McAnally et. al. (1986).

More information about the TABS models are given on the WWW page:

http://hlnet.wes.army.mil/software/tabs/tabs.htm

The most recent versions of the model is incorporated in the BOSS SMS system. It is running on PC's and workstations, and it is relatively inexpensive.

6.8 PHOENICS

The PHOENICS program is made by Cham Corporation. It was the first general-purpose CFD program, entering the marked in 1981. It is a finite volume program, using a structured non-orthogonal grid, and a staggered variable arrangement.

The program has been used for calculation of oil spill in the rivers of northern Russia, flow pattern in rivers (Oestberg and Johansson, 1992), flow in a channel (Toro et. al., 1989) and flow in settling tanks (Dahl et. al., 1994).

More information about PHOENICS is given on the WWW page:

http://www.cham.co.uk/

The most recent version of the program runs on UNIX and PC's. Several versions exist with prices from relatively inexpensive to relatively expensive.

An old version of the program is available as shareware and can be downloaded from the Internet.

6.9 CFX

CFX is a general-purpose CFD program owned by AEA Technology plc. It is a finite volume program. Two versions exist. CFX 4 uses structured multiblock non-orthogonal grids. CFX 5 uses an unstructured non-orthogonal grid.

CFX was previously called CFDS-FLOW3D.

The CFX program has previously been used for studying flow pattern in rivers together with pollution spreading, shown in the WWW page:

http://www.cad.oml.gov/cad_ce/text/mwq4.html

It has also been used by The Federal Institute of Technology, Lausanne, Switzerland, to calculate turbidity currents in a lake. An animation is given on the web page:

http://lchpc10.epfl.ch/cesare.html

More information about CFX is given on the WWW page:

http://www.aeat.co.uk/cfx/

The CFX program runs on UNIX workstations and it is relatively expensive.

7. Examples

Several examples are given in the following, reflecting possibilities for using CFD models in hydraulic and sedimentation engineering. Colour figures from the examples can be found on the World Wide Web at:

> http://www.sintef.no/nhl/vass/vassdrag.html
> http://www.bygg.ntnu.no/ivb/~nilsol/cfd

7.1 3D calculation of trap efficiency of a sand trap

The primary goal of the SSIIM model was to calculate sediment trap efficiency of an intake construction. One of the main parts of the intake is the sand trap. Olsen and Skoglund (1994) calculated the flow pattern and sediment trap efficiency for a sand trap, and verified the calculation with concentration measurements in a physical model study. The grid of the sand trap is shown in the figure below:
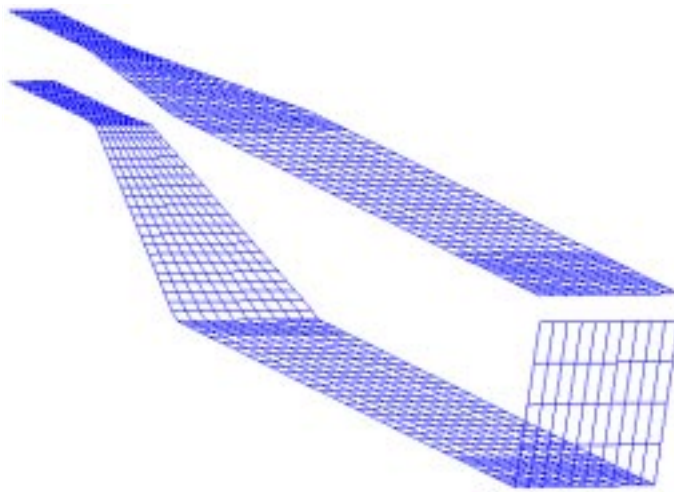
The figure to the right shows a 3D view of the grid along the bed and the surface, seen from the downstream upper side. The entrance is in the upper left corner, and the outlet in the lower right corner. There is an expansion region where the feeder channel flows into the sand trap. The expansion is both in the horizontal and vertical direction. A recirculation zone is formed at the expansion. To obtain the correct length of the recirculation zone, one of the constants in the k-ε model had to be slightly modified.
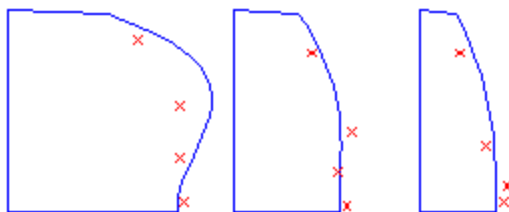
The figure to the left shows the measured and calculated concentration profiles in a longitudinal section. The lines are calculated concentrations and the crosses are measured values. There is fairly good agreement between the calculated and observed concentrations.

7.2 Sediment deposition and bed movements in a sand trap

The original trap efficiency calculation for the sand trap in Chapter 7.1 was for a steady situation. After some time, the sand trap will partly fill up with sediments before it is flushed. It is of interest to predict how the trap efficiency change as the sand deposit. This requires calculation of the vertical bed movements in the sand trap.

Olsen and Kjellesvig (1999) calculated sediment movements and bed changes in a tunnel-type sand trap. This was compared with results from a physical model study.
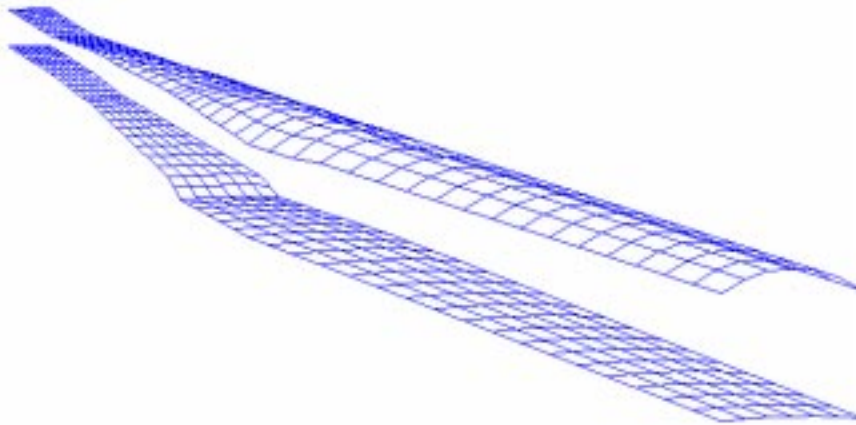
The figure above shows a 3D view of the grid along the bed and the roof. The upper left part of the figure is the entrance, and the lower right part is the outlet.
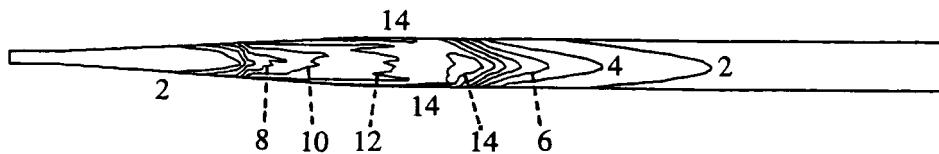

Water and sediments were added to the model and the bed elevation was measured. This compared fairly well with the calculated bed elevation. A contour map of the calculated bed elevation is given in the figure above, where the contour lines are given in cm.
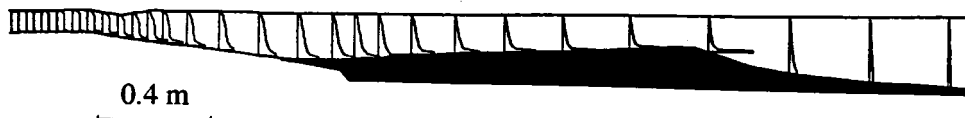
The figure above shows a longitudinal profile along the centreline of the flume with concentrations. The dark area is the deposited material.

7.3 Calculation of water and sediment flow in a hydropower reservoir

Just like the trap efficiency calculation is important for an intake, it is also important for smaller reservoirs. Water and sediment flow in the Garita Reservoir in Costa Rica was calculated by Olsen et. al. (1994). This is a small hydropower reservoir designed for daily peaking. The average depth of the reservoir is 5.5 meters, and the water discharge through the reservoir is 17 m^3/s. The figure below shows the depth-averaged velocity vectors.
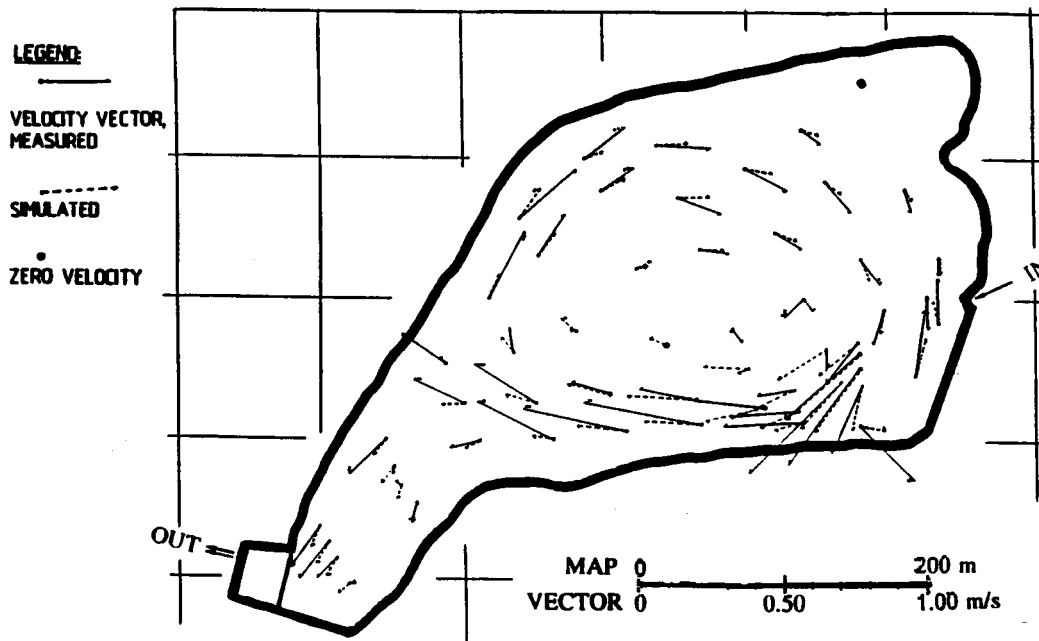
Olsen et. al. measured the velocities in the reservoir, and this is compared with the calculated velocities in the figure. The calculations captured all recirculation zones, and a parameter test with changes in the bed roughness did not influence the result. The sediment flow through the reservoir and the trap efficiency was also calculated, and it compared reasonably well with measurements.

7.4 Reservoir flushing

Sediment deposits in a reservoir can cause reduction in the effective storage volume and thereby an economic loss. For some cases, it has been possible to remove the sediments by flushing. Flushing is accomplished by lowering the water level at the dam, increasing the water velocity and causing erosion in the reservoir. It is of engineering and economic interest to be able to model the flushing process, to see how much sediments are removed and how the remaining sediments are distributed in the reservoir.

In the example shown here the flushing of the Kali Gandaki hydropower reservoir was simulated (Olsen, 1999). A physical laboratory model of this reservoir had been built, and could be used for verification of the numerical model. The model measured 5x11

meters and was built of concrete. Initially, a layer of sand with horizontal surface was laid on top of the bed. Water was then carefully filled into the model to avoid disruption of the sediments. When the water level was 15 cm. above the bed, the flushing started using a constant water discharge of 28 l/s. The downstream water level was lowered and the water flushed the sand forming a channel in the reservoir. After 2 ½ hours the test was stopped and the bed was measured.

The numerical model used a 2D depth-averaged water velocity calculation, together with a 3D solution of the convection-diffusion equation for sediment concentration.
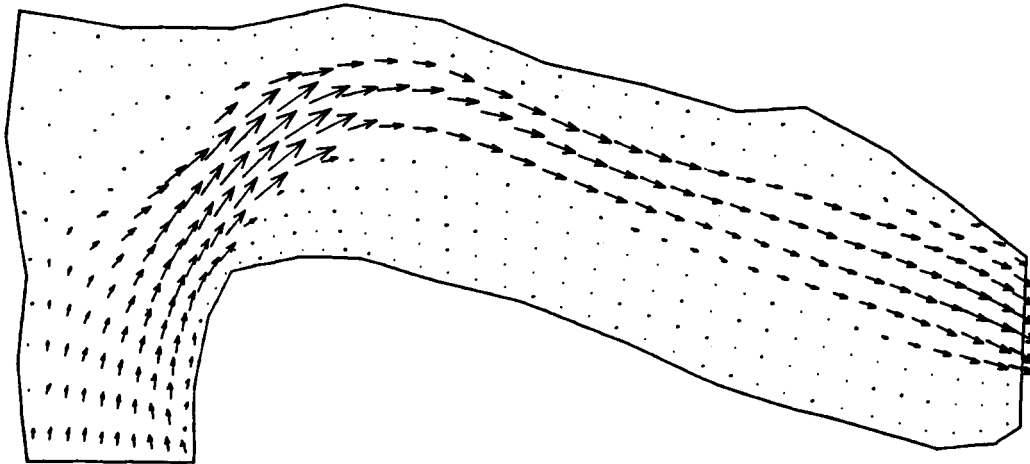
The figure above shows the calculated velocities after 2 ½ hours. The figure below shows a contour map of the calculated bed levels after 2 ½ hours, where the numbers are in cm above the spillway crest. There was reasonable agreement between measured and calculated bed elevations.
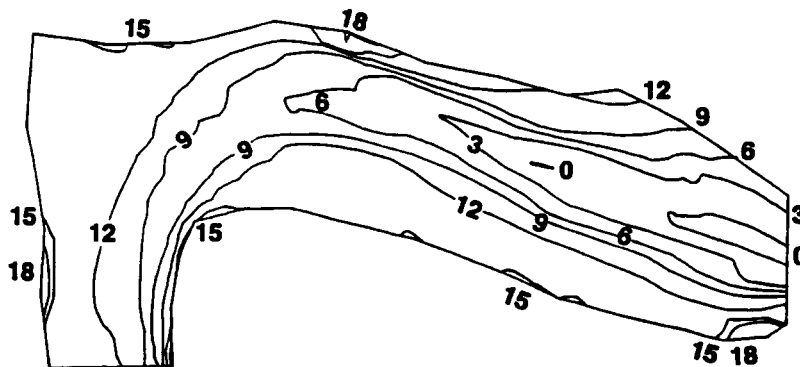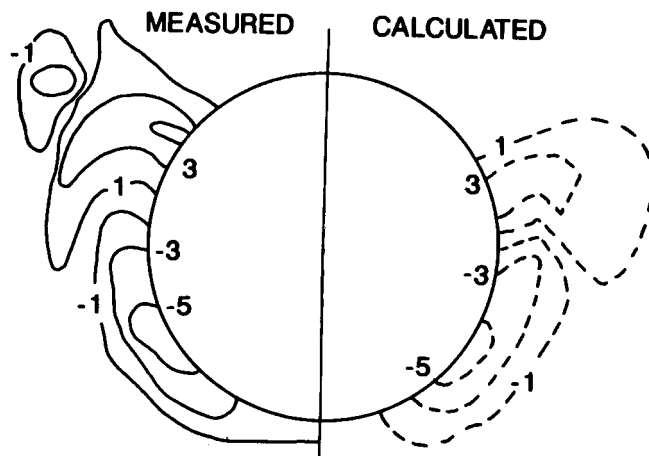
7.5 Local scour

Local scour is important for constructions in alluvial rivers. Much research has been done on bridge pier scour, because this has caused some bridges to collapse during floods.

Local scour around a bridge pier was calculated by Olsen and Melaaen (1993) and Olsen and Kjellesvig. In the first study only the shape of the scour hole was calculated, and the maximum scour depth was not calculated. This was however done in the second study. The figure below shows calculated and measured shape of the scour hole from the first study:

In this case a cylinder with diameter 75 cm was placed in a 3.65 m wide flume, covered with sediments. The sediments were plastic particles with density 1.04 and diameter 3 mm. The initial water depth was 33 cm and the upstream water velocity was 6.7 cm/s.

Calculated and measured scour hole, where the levels are given in cm.

More recently, Olsen and Kjellesvig (1998a) calculated local scour depth using the SSIIM model. A time-dependent calculation was done, where the Navier-Stokes equations and the sediment transport was calculated simultaneously. The depth of the emerging scour hole corresponded reasonably well with empirical formulas.

7.6 Turbidity current

Olsen and Tesaker (1995) calculated a turbidity current for a two-dimensional width-averaged situation. The numerical model reproduced a laboratory experiment with a turbidity current flowing inside a flume. It was necessary to modify the k-ε model to be able to simulate the decreased eddy-viscosity in the region above the current.

0.6 m/s: →
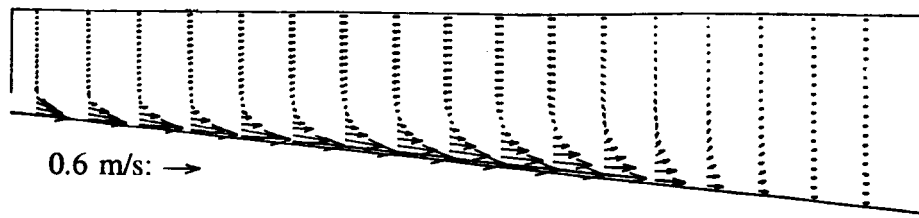
The velocity vectors in a longitudinal profile is shown in the figure above. The transient development of the calculated density current concentration is shown in the figure below.

6 sec.   12 sec.   18 sec.   24 sec.   30 sec.

· · · 30 sec.
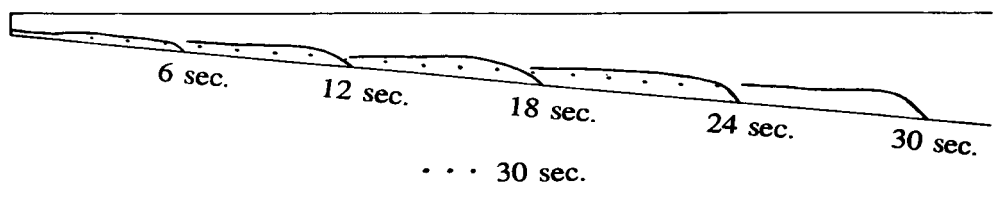
Turbidity current modelling has also been done for a fully 3D case, modelling a reservoir. This was done at EPFL, Lausanne, Switzerland, using the CFX model.

7.7 Spillway

Kjellesvig (1996) and Olsen and Kjellesvig (1997) calculated the coefficient of discharge for several spillways in two and three dimensions. The results were compared with experimental values and standard engineering literature. A time-dependent calculation was done with constant water discharge, starting with a horizontal water surface level. The water continuity in the cells closest to the water surface was used to update the adaptive grid. After convergence, the grid level behind the spillway was used to calculate the coefficient of discharge. The deviation between calculated and measured coefficient of discharge was 1% for the 3D case shown here. The water is flowing from left to right in the figure, showing the grid of the water surface and the bed.

The coefficient of discharge was also calculated by Yang and Johansson (1998) and Yang (1998) using a number of different commercial models: STAR-CD, PHOENICS, FLUENT and CFX. HR Wallingford has also calculated the coefficient of discharge for a spillway using FLOW-3D (Spaliviero and May, 1998). The spillway computation has also been done by Kruger et. al. (1998), using an in-house finite element program.

A similar phenomena is the computation of the Parshall Flume. The hydraulic jump downstream a control structure has also been modelled, for example by Richardson (1995).
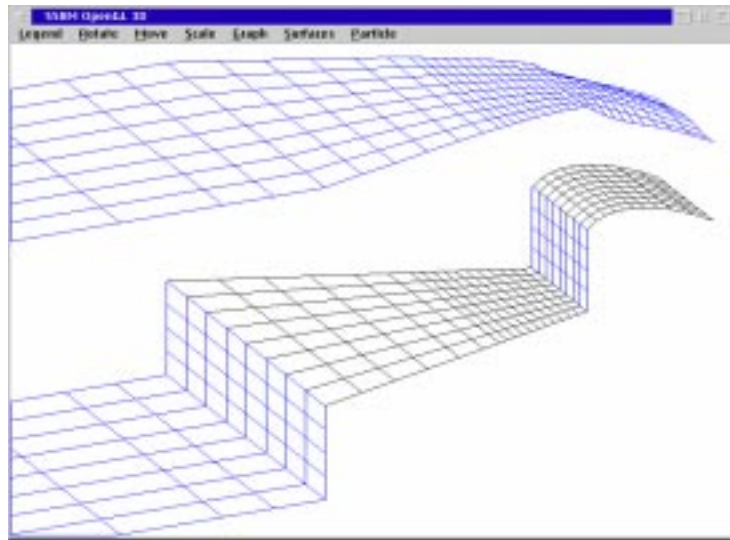
7.8 Flood wave

During the work on his doctoral dissertation, Løvoll (1996), Løvoll et. al (1995) investigated the forces on a construction being hit by a flood wave. The construction was a rectangular cylinder of 7x10 dm, located in a laboratory flume, 0.6 meter wide, 0.8 meter high and 26 meters long. The construction was hit by a flood wave with a water discharge between 34 and 160 litres/second. The figure below shows the calculated forces on the cylinder, compared with laboratory measurements.
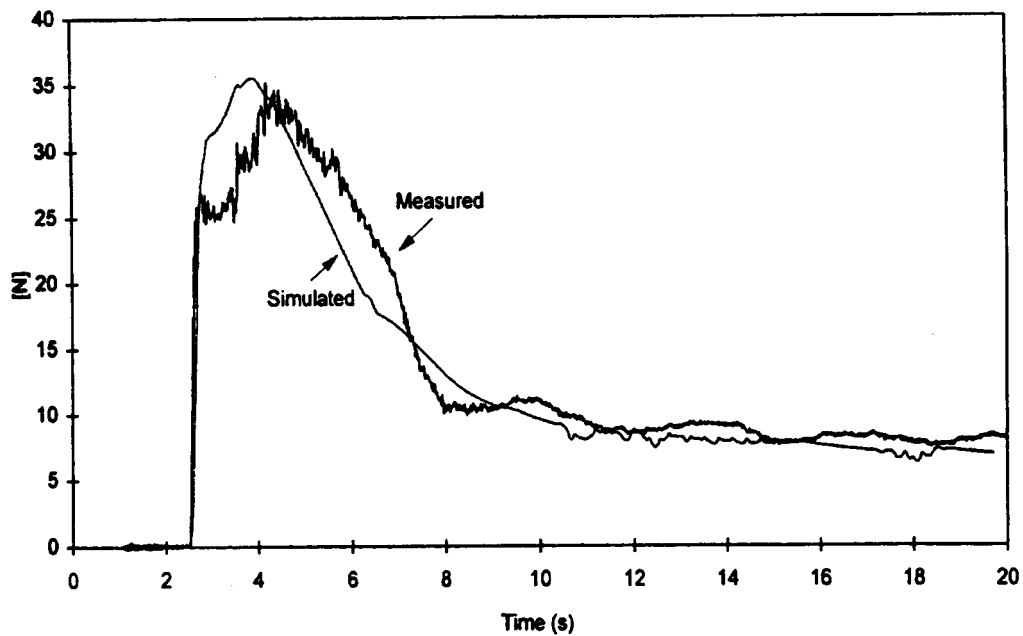
7.9 Flow pattern in rivers

Habitat studies in rivers often require an investigation of the flow pattern in a river with complex natural geometry. Olsen and Stokseth (1995) modelled a reach of Sokna river using a fully 3D model, where large rocks in the river were modelled as porosity. The porosity model was calibrated using measured velocities.

Alfredsen et. al. (1997) calculated both the location of the water surface and the water velocity in a river using two-dimensional depth averaged simulations. The programs SSIIM and AquaDyn were used. The results were transformed into habitat preferences for salmon and compared with measurements. The habitat preferences are shown in the figures below, where the upper figure shows the results from AquaDyn, and the lower figure shows the results from SSIIM:
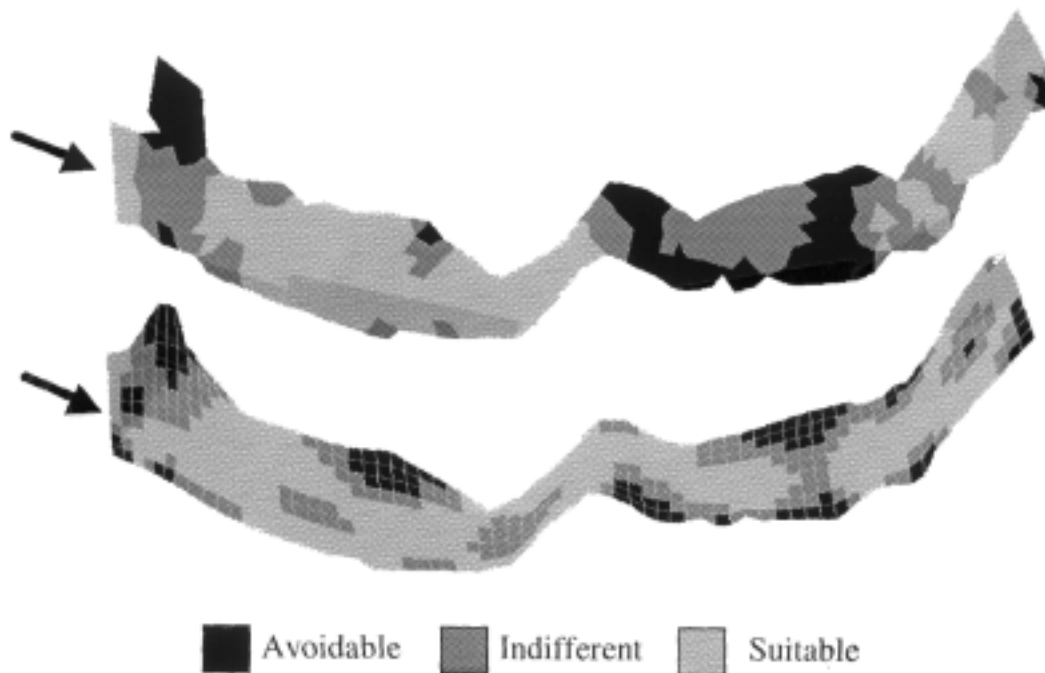
Over the last years, a number of other river reaches in Norway have been modelled by SINTEF for habitat studies. Further information is given on the web page:

http://www.sintef.no/units/civil/water/effekt/hydpeak.html

List of symbols

C_m, C_1, C_2	constants in the k-e model
c	concentration of sediments
D_*	parameter in van Rijn's formula for sediment concentration
d, d_s, d_{50}	mean diameter of sediment particle
d_{90}	diameter of sediment particle for which 90% is smaller
E	constant in wall function
g	acceleration of gravity
h	depth of water flow
k	turbulent kinetic energy
k_s	roughness at wall
M	Manning's friction coefficient
P	pressure
P_k	term for production of turbulence
Pe	Pechelet number
q_w	water discharge pr. unit width of canal
Sc	Schmidt number, ratio of turbulent eddy viscosity to sediment concentration diffusivity
T	parameter in van Rijn's formula for sediment concentration
U	average velocity
u	fluctuating velocity
u_*	shear velocity
x	coordinate
y	coordinate
z	coordinate

Greek

δ_{ij}	Kronecker delta: 1 if i=j, else zero
ε	dissipation rate of turbulent kinetic energy
Γ	turbulent diffusivity
κ	constant in wall function
ν	kinematic viscosity of water
ν_T	turbulent eddy viscosity
ρ_s	density of sediment
ρ_w	density of water
σ_k, σ_e	constants in the k-e equations
τ	shear stress

Literature

Ackers, P. and White, R. W. (1973) "Sediment Transport: New Approach and Analysis", ASCE Journal of Hydraulic Engineering, Vol. 99, No. HY11.

Alfredsen, K., Bakken, T. H., Harby, A. and Marchand, W. (1997) "Application and Comparison of Computer Models for Quantifying Impacts of River Regulations on Fish Habitat", HYDROPOWER '97, Trondheim, Norway.

Dahl, C., Larsen, T. and Petersen, O. (1994) "Numerical modelling and measurement in a test secondary settling tank", Water Science Technolgy, No. 2, pp. 219-228.

Einstein, H. A. (1950) "The Bed-Load Function for Sediment Transportation in Open-Channel Flows", Technical Bulletin no. 1026, US Department of Agriculture, Soil Conservation Service, Washington DC.

Engelund, F. and Hansen, E. (1967) "A monograph on sediment transport in alluvial streams", Teknisk Forlag, Copenhagen, Denmark.

Hervouet, J-M., Janin, J-M., Lepeintre, F. and Pechon, P. (1993) "TELEMAC-3D A Finite Element Software to Solve 3D Free Surface Problems", Int. Conf. on Advances in Hydroscience and Engineering, University of Mississippi, USA.

Keefer, T. N. (1971) "The relation of turbulence to diffusion in open-channel flow", PhD dissertation, Colorado State University, USA.

Kjellesvig, H. M. (1996) "Numerical modelling of flow over a spillway", Hydroinformatics-96, Zurich.

Kjellesvig, H. M. and Støle, H. (1996) "Physical and numerical modelling of the Himalaya Intake", 2nd Int. Conf. on Modelling, Testing and Monitoring for Hydro Powerplants, Lausanne, Switzerland.

Kruger, S., Burgisser, M. and Rutschmann, P. (1998) "Advances in calulating super-critical flow in spillway contractions", HYDROINFORMATICS '98, Copenhagen, Denmark.

Miller, A. C. (1971) "Turbulent diffusion and longitudinal dispersion measurements in a hydrodynamically rough open channel flow", PhD dissertation, Colorado State University, USA.

Naas, S. L. (1977) "Flow behavior in alluvial channel bends", PhD dissertation, Colorado State University, USA.

Løvoll, A., Lysne, D. K. and Olsen, N. R .B. (1995) "Numerical and physical modelling of dynamic impact on structures from a flood wave", IAHR 26th. Biennial Congress, London.

Løvoll, A. (1996) "Hydrodynamic forces in unsteady open channel flow", Dr. Ing. dissertation, Department of Hydraulic and Environmental Engineering, The Norwegian University of Science and Technology.

Lysne, D. K., Olsen, N. R. B., Støle, H and Jacobsen, T. (1995) "Withdrawal of water from sediment carrying rivers. Recent developments in planning and operation of headworks", International Journal on Hydropower and Dams, March.

McAnally, W. H. Jr., Letter, J. V. and Thomas, W. A. (1986) "Two and three-dimensional modeling systems for sedimentation", Third International Symposium on River Sedimentation, Jackson, USA.

Melaaen, M. C. (1992) "Calculation of fluid flows with staggered and nonstaggered curvilinear nonorthogonal grids - the theory", Numerical Heat Transfer, Part B, vol. 21, pp 1-19.

Oestberg, J. and Johansson, N. (1992) "Mathematical modelling of flow pattern", HYDROSOFT' 92, Valencia, Spain.

Olsen, N. R. B. (1991) "A numerical model for simulation of sediment movements in water intakes", Dr. Ing. Dissertation, The Norwegian Institute of Technology, Trondheim.

Olsen, N. R. B. and Melaaen, M. C. (1993) "Numerical Modeling of Erosion around a Cylinder and Sediment Deposition in a Hydropower Reservoir", Eight International Conference on Numerical Methods in Laminar and Turbulent Flow, Swansea, UK.

Olsen, N. R. B. and Melaaen, M. C. (1993) "Three-dimensional numerical modeling of scour around cylinders", ASCE Journal of Hydraulic Engineering, Vol. 119, No. 9, September.

Olsen, N. R. B., Jimenez, O., Lovoll, A. and Abrahamsen, L. (1994) "Calculation of water and sediment flow in hydropower reservoirs", IAHR International Conference on Modeling, Testing and Monitoring of Hydropower Plants, Hungary.

Olsen, N. R. B. and Alfredsen, K. (1994) "A three-dimensional model for calculation of hydraulic parameters for fish habitat", IAHR Conference on Habitat Hydraulics, Trondheim, Norway.

Olsen, N. R. B. (1994) "SSIIM - A three-dimensional numerical model for simulation of water and sediment flow", HYDROSOFT-94, Porto Carras, Greece.

Olsen, N. R. B. and Skoglund, M. (1994) "Three-dimensional numerical modeling of water and sediment flow in a sand trap", IAHR Journal of Hydraulic Research, No. 6.

Olsen, N. R. B. and Tesaker, E. (1995) "Numerical and physical modeling of a turbid-

ity current", IAHR 26th. Biennial Congress, London.

Olsen, N. R. B. and Oldervik, O. (1995) "Three-dimensional numerical modeling of water flow through a gate plug", IAHR 26th. Biennial Congress, London.

Olsen, N. R. B. and Stokseth, S. (1995) "Three-dimensional numerical modeling of water flow in a river with large bed roughness", IAHR Journal of Hydraulic Research, Vol. 33, No. 4.

Olsen, N. R. B. and Chandrashekhar, J. (1995) "Calculation of water and sediment flow in desilting basins", 6th. International Symposium on River Sedimentation, New Delhi, India.

Olsen, N. R. B. (1995) "Numerical modelling of hydropower reservoir flushing", International Conference on Hydropower into the next Century", Barcelona, Spain.

Olsen, N. R. B. and Melaaen, M. C. (1996) "Three-dimensional numeral modeling of transient turbulent flow around a circular cylinder", 2nd. Int. Conf. on Modelling, Testing and Monitoring for Hydro Powerplants, Lausanne, Switzerland.

Olsen, N. R. B. (1996) "Three-dimensional numerical modelling of local scour", Hydroinformatics-96, Zurich.

Olsen, N. R. B. (1997) "Computational fluid dynamics as a tool for prediction of sedimentation and erosion in reservoirs", Q. 74 a), ICOLD Conference, Florence, Italy.

Olsen, N. R. B. (1997) "A framework for a 3D numerical model for hydropower reservoir water quality", HYDROPOWER '97, Trondheim, Norway.

Olsen, N. R. B. and Kjellesvig, H. M. (1997) "A 3D numerical model for determination of spillway capacity", HYDROPOWER '97, Trondheim, Norway.

Olsen, N. R. B. and Kjellesvig, H. M. (1997) "3D Numerical Modelling of Sediment Deposition and Bed Changes in a Tunnel-Type Sand Trap", IAHR/ASCE Congress, San Francisco, USA.

Olsen, N. R. B. and Kjellesvig, H. M. (1998a) "Three-dimensional numerical flow modelling for estimation of maximum local scour depth", IAHR Journal of Hydraulic Research, No. 4.

Olsen, N. R. B. and Kjellesvig, H. M. (1998b) "Three-dimensional numerical flow modelling for estimation of spillway capacity", IAHR Journal of Hydraulic Research, No. 5.

Olsen, N. R. B. and Heslop, S. (1998) "Flow visualisation by particle animation for 3D CFD modelling in hydraulic engineering", HYDROINFORMATICS '98, Copenhagen, Denmark.

Olsen, N. R. B. (1998) "Unstructured and nested grids for 3D CFD modelling in hydraulic engineering", HYDROINFORMATICS '98, Copenhagen, Denmark.

Olsen, N. R. B. and Tjomsland, T. (1998) "3D CFD modelling of wind-induced currents and radioactive tracer movements in a lake", 3rd. International Conference on Hydroscience and Engineering, Cottbus, Germany.

Olsen, N. R. B., Hedger, R. D., George, D. G. and Heslop, S. (1998) "3D CFD modelling of spatial distribution of algae in Loch Leven, Scotland", 3rd. International Conference on Hydroscienceand Engineering, Cottbus, Germany.

Olsen, N. R. B. (1999) "Two-dimensional numerical modelling of flushing processes in water reservoirs", IAHR Journal of Hydraulic Research, Vol. 1.

Olsen, N. R. B. and Wilson, C. A. M. E. (1999) "CFD modelling of rivers and reservoirs", Int. Seminar on Optimum Operation of Run of River Reservoirs, Trondheim, Norway.

Olsen, N. R. B., Jimenez, O., Lovoll, A. and Abrahamsen, L. (1999) "3D CFD modelling of water and sediment flow in a hydropower reservoir", International Journal of Sediment Reserach, Vol. 14, No. 1.

Olsen, N. R. B. and Kjellesvig, H. M. (1999) "Three-dimensional numerical modelling of bed changes in a sand trap", IAHR Journal of Hydraulic Research, Vol. 37, No. 2. abstract

Olsen, N. R. B. and Lysne, D. K. (1999) "3D Numerical Modelling of Water Currents in an Ice-Covered Lake", IAHR 28th. Bienneal Congress, Graz, Austria.

Olsen, N. R. B., Hedger, R. D. and George, D. G. (1999) "Modelling the Horizontal Distribution of Algae in a Water Supply Reservoir", IAHR 28th. Bienneal Congress, Graz, Austria.

Patankar, S. V. (1980) "Numerical Heat Transfer and Fluid Flow", McGraw-Hill Book Company, New York.

van Rijn, L. C. (1987) "Mathematical modeling of morphological processes in the case of suspended sediment transport", Ph.D Thesis, Delft University of Technology.

Rhie, C.-M, and Chow, W. L. (1983) "Numerical study of the turbulent flow past an airfoil with trailing edge separation", AIAA Journal, Vol. 21, No. 11.

Richardson, J. E. (1997) "Control of Hydraulic Jump by Abrupt Drop," XXVII IAHR Congress, San Francisco, USA.

Rodi, W. (1980) "Turbulence models and their application in hydraulics", IAHR State-of-the-art paper.

Rouse, H (1937) "Modern Conceptions of the Mechanics of Fluid Turbulence", Transactions, ASCE, Vol. 102, Paper No. 1965.

Seed, D. (1997) "River training and channel protection - Validation of a 3D numerical model", Report SR 480, HR Wallingford, UK.

Sintic, A. (1996) "Numerical models for dam-break flood routing", MS Thesis, Institute of Hydraulic Engineering and Water Resources Management, University of Technolgy, Aachen, Germany.

Spaliviero, F. and May, R. (1998) "Numerical modelling of 3D flow in hydraulic structures", IAHR/SHSG seminar on Hydraulic Engineering, Glasgow, UK.

Stoesser, T. (1998) "Numerical Modelling as Tool in Hydraulics - In Case of Reservoir Sedimentation Processes in Mountainous Regions", Dipl. Ing. Thesis, Institute of Hydraulic Engineering and Water Resources Mangagement, University of Karlsruhe, Germany.

Schlichting, H. (1979) "Boundary layer theory", McGraw-Hill.

Tamamidis, P. and Assanis, D. N. (1993) "Evaluation of various high-order accuracy schemes with and without flux limiters", International Journal for Numerical Methods in Fluids, Vol. 16, pp. 931-948.

Taylor, C. and Huges, T. G. (1981) "Finite element method for the Navier-Stokes equations", Pineridge Press Limited.

Toro, F. M., Meijer, K. and van Rijn, L. (1989) "Quasi-3D and Fully-3D Modelling of Suspended Sediment Transport", ASCE Hydraulics Conference, New Orleans.

Vanoni, V., et al (1975) "Sedimentation Engineering", ASCE Manuals and reports on engineering practice - No54.

White, F. M. (1974) "Viscous Fluid Flow", McGraw-Hill Book Company.

Yang, J. and Johansson, N. (1998) "Determination of Spillway Discharge Capacity - CFD Modelling and Experimental Verification", HYDROINFORMATICS '98, Copenhagen, Denmark.

Yang, J. (1998) Personal communication.